JAERI-M
9695

PALLAS-PL,SP-Br : A CODE FOR DIRECT INTEGRATION OF TRANSPORT EQUATION IN ONE-DIMENSIONAL PLANE AND SPHERICAL GEOMETRIES

September 1981

Kiyoshi TAKEUCHI* and Shun-ichi TANAKA

日本原子力研究所
Japan Atomic Energy Research Institute

JAERI-M 9695

PALLAS-PL,SP-Br : A Code for Direct Integration of Transport Equation in One-Dimensional Plane and Spherical Geometries

Kiyoshi TAKEUCHI* and Shun-ichi TANAKA
Division of Reactor Engineering, Tokai Research Establishment, JAERI

(Received September 3, 1981)

The PALLAS-PL,SP-Br program is the revised version of the old PALLAS-PL,SP code which has been developed in 1973 on the basis of a method of direct integration of the Boltzmann transport equation to describe neutron transport in one-dimensional plane and spherical geometries. The revised version can treat transport of both neutrons and gamma rays, in particular of secondary gamma rays including the bremsstrahlung and the annihilation photons. The document gives a full description of theoretical calculation, input and output data, as well as code implementation information and a description of several demonstration problems.

Keywords : Revised PALLAS-PL,SP Code, Direct Integration Method, One-Dimensional Plane and Spherical Geometries, Neutron and Gamma Rays Transport, Bremsstrahlung and Annihilation Photons

---

* On leave from Ship Research Institute

PALLAS－PL, SP－Br：1次元平板および球形状における輸送方程式の直接積分コード

日本原子力研究所東海研究所原子炉工学部
竹内　清*・田中俊一

（1981年9月3日受理）

1次元平板および球形状において中性子の輸送計算を行うため，1973年に開発されたボルツマン輸送方程式の直接積分コード：PALLAS－PL，SPが改良されPALLAS－PL，SP－Brコードが新たに作成された。後者のコードでは中性子の他にガンマ線の輸送計算，特に中性子の反応によって生じる2次ガンマ線や制動輻射線や消滅ガンマ線を含む2次ガンマ線の輸送計算が可能である。本報告には，PALLAS－PL，SP－Brコードの理論式，コードの入出力データおよびコード使用の際に必要な情報と，幾つかの計算例が述べられている。

*協力研究員（船舶技術研究所）

Contents

1. Program Abstract 1
2. Introduction 3
3. Theory 5
(1) Evaluation of the source term Q (r,ω,E) 5
(2) Calculation of the integral transport equation .. 11
(3) New technique for treatment of the within-group scattering 14
(4) Secondary gamma-ray source produced by neutron reaction 16
(5) Annihilation gamma-ray source 16
(6) Bremsstrahlung photon source 17
(7) Slowing down calculation into thermal group and convergence 22
(8) Mono-energy source calculation 23
4. Restriction of Input Data 27
5. Program Structure 27
6. Information for Users 28
6.1 Input Specification 28
6.2 Detailed Data Notes 36
6.3 Special Notes 40
(1) Spatial mesh assignment 40
(2) Secondary Gamma-ray energy structure fixed in the code 40
(3) Angular quadrature sets 40
(4) PALLAS neutron library 41
(5) PALLAS gamma-ray library 42
6.4 External and Internal Data Files 43
6.5 Main Program Variables and Program Mnemonics 43
6.6 Sample Problems 44
Acknowledgement 47
References 47

目　　次

1. プログラムの概要 …… 1
2. 序　　言 …… 3
3. 計算コードの理論式 …… 5
   (1) 線源項の計算 …… 5
   (2) 直接積分方程式の計算 …… 11
   (3) 自群散乱取扱いの新しい方法 …… 14
   (4) 中性子による2次ガンマ線線源 …… 16
   (5) 消滅ガンマ線線源 …… 16
   (6) 制動輻射によるガンマ線線源 …… 17
   (7) 熱中性子群への減速計算と収束条件 …… 22
   (8) 単色エネルギ線源に対する計算 …… 23
4. 入力データの制限条件 …… 27
5. プログラムの構成 …… 27
6. 使用者のための情報 …… 28
   6.1 入力データの作成法 …… 28
   6.2 入力データについての詳細な説明 …… 36
   6.3 特別の注意事項 …… 40
   (1) 空間メッシュの取り方 …… 40
   (2) コード内で決められる2次ガンマ線のエネルギ群構造 …… 40
   (3) 角度分点セット …… 40
   (4) PALLAS用中性子ライブラリィ …… 41
   (5) PALLAS用ガンマ線ライブラリィ …… 42
   6.4 データファイル使用法 …… 43
   6.5 コード内で使用している主な変数の意味 …… 43
   6.6 例　　題 …… 44
   謝　　辞 …… 47
   参考文献 …… 47

1. Program Abstract

(1) Name of Program: PALLAS-PL,SP-Br

(2) Computer for which designed or operable: FACOM M-200 and IBM 370/168

(3) Nature of physical problem solved: PALLAS-PL,SP-Br solves the steady state Boltzmann transport equation in one-dimensional plane and spherical geometries. It can solve also the transport of secondary gamma rays such as bremsstrahlung and annihilation photons. Application is restricted to a fixed-source problem.

(4) Method of solution: The method of direct integration of the transport equation is used, in which the equation is integrated along the flight path of radiation in the direction of motion at each discrete ordinate direction. Anisotropic scattering is treated precisely using differential scattering cross sections for elastic scattering, however isotropic scattering in the laboratory system is assumed in inelastic scattering of neutron. No iteration and convergence techniques are used for obtaining the flux.

(5) Restriction: About 400K words are required for the total core storage for 70 spatial, 30 angular and 45 energy meshes in bremsstrahlung transport calculations.

(6) Usual features: Fixed dimensioning is used, so that always 200K core storage is required for no bremsstrahlung transport calculation. Nuclear data for neutron and secondary gamma rays are read in from the PALLAS library tape (or disk). Coefficients for linear attenuation, pair production and photoelectric effect of gamma rays are interpolated for specified energies from the PALLAS gamma-ray library in the code, where the data for discrete energies from 0.01 to 20 MeV are given for the same nuclides and materials as those of neutrons. Similarly, the flux to dose conversion

fator for exposure dose, dose equivalent and absorbed dose alse are interpolated.

(7) Special features: The differential electron production cross sections relating to the pair production reaction are calculated within the code, also the differential bremsstrahlung gamma-ray production cross sections and the stopping power are calculated within the code.

(8) Typical running time: About 0.0009 sec/spatial mesh/group is required as cpu time on FACOM M-200.

(9) Machine requirements: Card input, printed output, and scratch data sets may be located on defined external storage device.

(10) Language: FORTRAN IV

(11) Material available: Input description, source deck for FORTRAN routines and sample problems.

2. Introduction

The PALLAS-PL, SP-Br computer programme solves the energy and angular dependent Boltzmann transport equation with general anisotropic scattering in plane and spherical geometries. Principal applications are to neutron and gamma-ray transport problems in forward mode. The code is particularly designed and suited to the solution of radiation shielding problems with external source.

The code has been designed based on a method of direct integration of the transport equation[1)2)], in which the equation is solved by integrating along a flight path of radiation in the direction of motion at each discrete-ordinate angle. The specific features of this method are that (1) the radiation flux is calculated at each energy mesh ($n/cm^2 \cdot sec \cdot (sr) \cdot MeV$) without using any conventional iterative techniques used widely in Sn method for obtaining group flux at each energy group, and (2) the scattering calculations are made directly using the differential scattering cross section for neutron and the Klein-Nishina formula for gamma ray[3)]. Thus a Legendre polynomial expansion approximation used widely in Sn method is not applied to the calculation of radiation scattering. As a result the PALLAS can provide always positive and physically meaningful angular and scalar fluxes. Besides, (3) no supplementary difference equations are required to obtain a solution to the flux, which makes users free from bothering about choice of such modes as "diamond difference", "step function" and "weighted difference" equations. By virtue of no usage of average flux, the PALLAS can be applied to even such problems as violently varied angular and spatial distributions of radiation flux[4)]. In contrast, one-dimensional Sn codes calculate the transport equation based on the average flux for a cell with each pair of associated cell face fluxes in the three-dimensional finite cells defined in terms of location, direction,

and energy phase space variables. The most underlined feature is to deal with transport of secondary photons produced by reactions of bremsstrahlung and annihilation[5].

The weak point in the present PALLAS-PL,SP-Br code is that it has been written in the fixed dimensioning, which restricts the numbers of energy meshes, material regions, nuclides, angular meshes, spatial meshes to be inputed.

Both the neutron and secondary gamma-ray production cross sections for PALLAS-PL,SP-Br are taken from the PALLAS neutron library. The gamma-ray cross sections are also taken from the PALLAS gamma library, however gamma-ray scattering cross sections are not required by virtue of direct use of the Klein-Nishina formula. Both the data for electron production resulting from pair creation reaction and for bremsstrahlung photon production are calculated in the PALLAS-PL,SP-Br code.

The original PALLAS-PL,SP code was written for IBM 360 computer in 1973[6] to calculate neutron transport in shields. Revisions have been made to the old version so as to calculate transport of gamma rays including bremsstrahlung and annihilation photons as well as secondary photons resulting from neutron reaction.

3. Theory

The steady-state radiation transport equation is written with usual notations as

$$\bar{\Omega}\nabla\Phi + \Sigma_t(\bar{r},E)\Phi(\bar{r},\bar{\Omega},E) = \int\int dE'd\bar{\Omega}'\ \Phi(\bar{r},\bar{\Omega}',E')\Sigma_s(\bar{r},E'\to E,\bar{\Omega}'\to\bar{\Omega}) + S(\bar{r},\bar{\Omega},E). \quad (1)$$

The above equation can be rewritten in the following integral form on the basis of a condition of a constant total cross section within any spatial interval $(\bar{r}',\bar{r})$:

$$\Phi(\bar{r},\bar{\Omega},E) = \Phi(\bar{r}',\bar{\Omega},E)\exp(-\Sigma_t R) + \int_0^R Q(\bar{r}",\bar{\Omega},E)\exp(-\Sigma_t R')dR', \quad (2)$$

where $R=|\bar{r}-\bar{r}'|$, $R'=|\bar{r}-\bar{r}"|$ and $\bar{r}"=\bar{r}-R'\bar{\Omega}$, and $\Sigma_t\equiv\Sigma_t(\bar{r}",E)=$ constant. Further,

$$Q(\bar{r},\bar{\Omega},E) = \int\int\Sigma_s(\bar{r},E'\to E,\bar{\Omega}'\to\bar{\Omega})\Phi(\bar{r},\bar{\Omega}',E')d\bar{\Omega}'dE' + S(\bar{r},\bar{\Omega},E). \quad (3)$$

The direction of radiation flight $\bar{\Omega}$ is represented by discrete-ordinate directional meshes ω_p ($\omega=\cos\theta$ and θ is the polar angle).

(1) Evaluation of the source term $Q(\bar{r},\omega,E)$

In order to perform numerical integration of the first term on the right hand side of Eq.(3), the flux is transformed into the energy flux $I(\bar{r},\omega,E)$:

$$I(\bar{r},\omega,E) = E\Phi(\bar{r},\omega,E).$$

The differential scattering cross section is represented by

$$\Sigma_s(\bar{r},E'\to E,\bar{\Omega}'\to\bar{\Omega}) = \Sigma_{el}(\bar{r},E')f_{el}(E',\mu)\delta(\cos\theta-\alpha)\frac{(A+1)^2}{2AE'} \quad (4)$$

for neutron elastic scattering,

$$= \Sigma_{in}(\bar{r},E')\ \frac{f_{in}(E'\to E)}{4\pi} \quad (5)$$

for neutron inelastic scattering,

$$= n(\bar{r})\frac{d\sigma}{d\Omega}(E',\theta)\frac{m_0c^2}{E^2}\delta(\cos\theta-\alpha) \quad (6)$$

for photon compton scattering,

where $\Sigma_{el}(\bar{r},E)$ and $\Sigma_{in}(\bar{r},E)$ are respectively the total elastic and inelastic scattering cross sections, A is the mass number of nuclide and μ is the cosine of the polar angle of elastic scattering in the center of mass system, while α is the cosine of the same angle in the laboratory system. The azimuthal angle of elastic scattering is represented by ψ. Further, $f_{el}(E,\mu)$ is the scattering distribution function and is normalized to 1.0 as

$$2\pi\int_{-1}^{1} f_{el}(E,\mu)d\mu = 1, \tag{7}$$

and $f_{in}(E'\rightarrow E)$ is the slowing down probability assuming that the inelastic scattering is isotropic in the laboratory system.

For Compton scattering the cross section is exactly represented by the Klein-Nishina formula, so that the scattering kernel K(E',E) is derived from the Klein-Nishina formula: The Klein-Nishina formula is expressed in terms of energy or the Compton wavelength as

$$\frac{d\sigma}{d\Omega} = \frac{3}{16\pi}\mu_T\left(\frac{E}{E'}\right)^2\left(\frac{E}{E'} + \frac{E'}{E} - \sin^2\theta\right), \tag{8}$$

or

$$\frac{d\sigma}{d\Omega} = \frac{3}{16\pi}\mu_T\left(\frac{\lambda'}{\lambda}\right)^2\left(\frac{\lambda'}{\lambda} + \frac{\lambda}{\lambda'} - \sin^2\theta\right), \tag{9}$$

where the Compton wavelength is given by

$$\lambda = \frac{m_0c^2}{E(MeV)} = \frac{0.511}{E}, \tag{10}$$

and μ_T=0.665 (barns/electron).

Consequently the scattering kernel K(E',E) is used in the expression (6), written as

$$K(E',E) = \frac{3}{8}\mu_T\left(\frac{E}{E'}\right)\left(\frac{E}{E'} + \frac{E'}{E} - \sin^2\theta\right). \tag{11}$$

There is a relation between the energy variation and scattering angle:

$$E = \frac{E'}{1+(E'/m_0c^2)(1-\cos\theta)}, \tag{12}$$

thus

$$-\sin^2\theta = -1+\cos^2\theta$$
$$= 2\left(\frac{m_0c^2}{E'} - \frac{m_0c^2}{E}\right) + \left(\frac{m_0c^2}{E'} - \frac{m_0c^2}{E}\right)^2. \tag{13}$$

The expression (11) is rewritten as

$$K(E',E) = \frac{3}{8}\mu_T\left(\frac{E}{E'}\right)\left[\frac{E}{E'} + \frac{E'}{E} + 2\left(\frac{m_0c^2}{E'} - \frac{m_0c^2}{E}\right) + \left(\frac{m_0c^2}{E'} - \frac{m_0c^2}{E}\right)^2\right], \tag{14}$$

and further

$$K(\lambda',\lambda) = \frac{3}{8}\mu_T\left(\frac{\lambda'}{\lambda}\right)\left[\frac{\lambda}{\lambda'} + \frac{\lambda'}{\lambda} + 2(\lambda'-\lambda) + (\lambda'-\lambda)^2\right]. \tag{15}$$

The remaining unknown variable n(r) in the expression (6) is the electron density.

In the subsequent discussion the spatial variable $\bar{r}$ is expressed by x. The neutron elastic scattering source $Q^N_{el}(x,\omega,E)$ is written in terms of energy flux as

$$Q^N_{el}(x,\omega,E) = \int\int\int \Sigma_{el}(x,E')f_{el}(E',\mu)\delta(\cos\Theta-\alpha) \frac{(A+1)^2}{2AE'}\cdot\frac{E}{E'}I(x,\omega',E')d\alpha d\psi dE'. \tag{16}$$

From the relation between μ and E of

$$\mu = 1 - \frac{(A+1)^2}{2A}\left(1 - \frac{E}{E'}\right), \tag{17}$$

$$dE' = \frac{2A}{(A+1)^2}\frac{E'^2}{E}d\mu. \tag{18}$$

Then the above expression (16) is rewritten as

$$Q^N_{el} = \int\int \Sigma_{el}(x,E')f_{el}(E',\mu)I(x,\omega',E')d\mu d\psi. \tag{19}$$

Numerical integration on μ is carried out by using Gaussian quadrature, in which $f_{el}(E',\mu)$ is represented by $f^m(E')$ at discrete meshes $\mu_m(m=1,2,---,M)$. In order to carrying out the numerical integration over the azimuthal angle ψ, we represent

it by finite mesh points ψ_n (n=1,2,---,Q) in accordance with the meshes ω_q (q=1,2,---,Q) defining the discrete angular points of radiation moving direction (Fig.1). The relationship between the scattering polar angle and azimuthal angle is represented by

$$\cos\theta' = \cos\theta\cos\Theta + [(1-\cos^2\theta)(1-\cos^2\Theta)]^{1/2}\cos\psi, \tag{20}$$

and then

$$\omega' = \omega\alpha + [(1-\omega^2)(1-\alpha^2)]^{1/2}\cos\psi. \tag{21}$$

Here θ' and θ are the direction angles of radiation before and after scattering. Further Θ and α are the scattering angle and its cosine ($\alpha=\cos\Theta$), respectively.

When we define $\mu=\mu_m$, then α_m is determined from

$$\alpha_m = \frac{A\mu_m+1}{(A^2+2A\mu_m+1)^{1/2}}. \tag{22}$$

Consequently ψ_n is determined using the relations of (21) and (22) for a certain direction $\omega=\omega_p$ as

$$\psi_n \equiv \psi(\omega_n,\omega_p,\alpha_m) = \cos^{-1}\{\frac{\omega_n-\omega_p\alpha_m}{[(1-\omega_p^2)(1-\alpha_m^2)]^{1/2}}\}. \tag{23}$$

The weight for ψ_n is defined by

$$w_n = |\psi(\omega_n^u,\omega_p,\alpha_m) - \psi(\omega_n^\ell,\omega_p,\alpha_m)|, \tag{24}$$

where ω_n^u and ω_n^ℓ are the values of upper and lower bounds of ω_n range respectively.

Now the expression (19) can be numerically evaluated for $\omega=\omega_p$ at x as

$$Q_{el}^N(x,\omega_p,E) = \sum\sum_{mn} W_m w_n \Sigma_{el}(x,E_{(m)}) f^m(E_{(m)}) I(x,\omega_n,E_{(m)}), \tag{25}$$

where W_m is the weight for $\mu=\mu_m$ in the Gaussian quadrature, and $E_{(m)}$ is determined for $E=E_j$ and $\mu=\mu_m$ from

$$E_{(m)} = \frac{(A+1)^2}{A^2+2A\mu_m+1} E_j. \tag{26}$$

For simplicity in practical calculations, both the radiation flux and source at the energy point $E_{(m)}$ are chosen in the following manner. First, the energy mesh E_j is basically chosen at a midpoint of the E_j energy region, except for the energy mesh E_{j-1} which is just above the energy mesh E_j of interest. The energy region of E_{j-1} is defined as illustrated in Fig.2, which is for the purpose of avoiding the use of iterative calculation for obtaining radiation flux. Then if $E_{(m)}$ determined by Eq.(26) belongs to the energy region of k-th energy mesh E_k, the values of $\Sigma_{el}(E_k)$, $f^m(E_k)$ and $I(E_k)$ are chosen for those of $\Sigma_{el}(E_{(m)})$, $f^m(E_{(m)})$ and $I(E_{(m)})$.

The neutron inelastic scattering source Q^N_{in} is numerically evaluated on the basis of an assumption of isotropic scattering in the laboratory system:

$$Q^N_{in}(x,\omega,E) = \int \Sigma_{in}(x,E') \frac{f_{in}(x,E',E)E}{4\pi E'} I_0(x,E')dE', \tag{27}$$

where

$$I_0(x,E') = 2\pi \int I(x,\omega,E')d\omega. \tag{28}$$

The expression(27) is readily calculated for the energy mesh E_j as

$$Q^N_{in}(x,\omega,E_j) = \sum_{k=1}^{j-1} \Sigma_{in}(x,E_k) \frac{f_{in}(E_k,E_j)E_j}{4\pi E_k} I_0(x,E_k)\Delta E_k$$

$$= \sum_{k=1}^{j-1} \frac{\Sigma_{in}(E_k,E_j)E_j}{4\pi E_k} I_0(x,E_k)\Delta E_k, \tag{29}$$

where $\Sigma_{in}(E_k,E_j)$ is the macroscopic differential inelastic scattering cross section for each nuclide.

The gamma-ray scattering source is evaluated based on the Klein-Nishina formula, which is written in terms of energy flux as

$$Q^G(x,\omega,E) = \int\int n(x)\frac{d\sigma}{d\bar{\Omega}}\frac{m_0c^2}{E^2}\left(\frac{E}{E'}\right)\delta(\cos\theta-\alpha)I(x,\omega',E')d\bar{\Omega}'dE' \tag{30}$$

$$= \int\int n(x)\frac{d\sigma}{d\bar{\Omega}}\frac{m_0c^2}{E^2}\left(\frac{E}{E'}\right)I(x,\omega',E')d\psi dE'$$

$$= \int\int n(x)\frac{K(E',E)}{2\pi}I(x,\omega',E')\frac{m_0c^2}{E'^2}d\psi dE' \tag{31}$$

or

$$Q^G(x,\omega,\lambda) = \int\int n(x)\frac{d\sigma}{d\bar{\Omega}}\cdot\frac{m_0c^2}{E^2}\cdot\left(\frac{E}{E'}\right)I(x,\omega,\lambda')d\psi\left(\frac{E'}{\lambda'}\right)d\lambda'$$

$$= \int\int n(x)\frac{1}{2\pi}\left(\frac{\lambda'}{\lambda}\right)K(\lambda',\lambda)\left(\frac{\lambda}{E}\right)\left(\frac{E}{E'}\right)I(\lambda')\left(\frac{E'}{\lambda'}\right)d\psi d\lambda'$$

$$= \int\int n(x)\frac{K(\lambda',\lambda)}{2\pi}I(x,\omega',\lambda')d\psi d\lambda' \tag{32}$$

The integration over ψ is carried out in the same way as in the neutron elastic scattering integral calculation. In the gamma-ray calculation $\alpha_m=\mu_m$ and $\mu_m=1+\lambda_m-\lambda$. Consequently

$$\psi \equiv \psi(\omega_n,\omega_p,\mu_m) = \cos^{-1}\left\{\frac{\omega_n-\omega_p\mu_m}{[(1-\omega_p^2)(1-\mu_m^2)]^{1/2}}\right\}, \tag{33}$$

and

$$w_n = |\psi(\omega_n^u,\omega_p,\mu_m)-\psi(\omega_n^\ell,\omega_p,\mu_m)|. \tag{34}$$

Numerical integration of Eq.(32) yields

$$Q^G(x,\omega_p,\lambda_j) = \sum_{kn}\sum w_n\, n(x)\frac{K(\lambda_k,\lambda_j)}{2\pi}I(x,\omega_n,\lambda_k)\Delta\lambda_k. \tag{35}$$

From the calculations described above, the source term $Q(x,\omega,E)$ is numerically evaluated for a set of discrete meshes ($x=x_i$, $\omega=\omega_p$ and $E=E_j$) as

$$Q(x_i,\omega_p,E_j) = Q_{el}^N(x_i,\omega_p,E_j) + Q_{in}^N(x_i,\omega_p,E_j) + S(x_i,\omega_p,E_j) \tag{36}$$

for neutron,

$$= Q^G(x_i,\omega_p,\lambda_j) + S(x_i,\omega_p,E_j) \quad (37)$$

for gamma ray,

where $S(x,\omega,E_j) = E_j s(x,\omega,E_j)$, (38)

and s and S are respectively the external source and energy source. Consequently the neutron source term can be evaluated from the expressions (25) and (29), and the gamma-ray source term can be evaluated from the expression (35).

(2) Calculation of the integral transport equation

Since the source term $Q(x,\omega,E)$ has been numerically evaluated in the previous section, Eq.(2) can be numerically calculated. The equation (2) is rewritten in terms of energy flux in one-dimensional geometry as

$$I(x,\omega,E) = I(x',\omega,E)\exp(-\Sigma_t R) + \int_0^R Q(x'',\omega,E)\exp(-\Sigma_t R')dR'. \quad (39)$$

First, the spatial variable is partitioned into x_i (i=1,2,---, MRR), in which the cross section is constant in any spatial intervals (x_{i-1},x_i). Next, the source term Q must be approximated by some simple functions with respect to x so that the integration over R' can be carried out. In the original PALLAS-PL,SP code, a linear function approximation with respect to x has been applied. Later N.Sasamoto has introduced an exponential approximation[4] for this function in order to yielding more accurate solutions in attenuating media in shields even in the case of rather rough spatial mesh intervals.

The former approximation enables us to perform numerical calculation of the integration over R':

$Q(x'',\omega,E) \equiv Q(x'') = a+bR'$,

then

$$\int_0^R (a+bR')\exp(-\Sigma_t R')dR' = \frac{1}{\Sigma_t^2 R}\{Q(x_i)[\Sigma_t R + \exp(-\Sigma_t R) - 1]$$

$$+ Q(x_{i-1})[1-(1+\Sigma_t R)\exp(-\Sigma_t R)]\}. \qquad (40)$$

On the other hand, the latter approximation results in

$$Q(x",\omega,E) \equiv Q(x") = a\cdot\exp(bR'),$$

then

$$\int_0^R a\cdot\exp(bR')\exp(-\Sigma_t R')dR' = \frac{[Q(x_{i-1})\exp(-\Sigma_t R)-Q(x_i)]R}{\ln\frac{Q(x_{i-1})}{Q(x_i)} - \Sigma_t R}. \qquad (41)$$

Since the first term on the right hand side of Eq.(39) is an analytical expression, the numerical error in a solution of the integral transport equation depends on that of the numerical integration of the second term. In the current PALLAS-PL,SP code, the choice of the expression (40) or (41) is determined depending upon the ratio of $Q(x_{i-1})/Q(x_i)$ except for $Q(x_i)=0$: For $1/2 \leq Q(x_{i-1})/Q(x_i) \leq 2$, the expression (40) is automatically chosen in the code, while for ratios other than the above range the expression (41) is chosen. In the case of $Q(x_i)=0$, the expression (40) is chosen in the code.

From the integral calculation described above, the integral transport equation (39) is calculated, which is written with the notation of the energy flux in one-dimensional plane or spherical geometry as

$$I(x_i,\omega_p,E_j) = I(x_{i-1},\omega_p,E_j)\exp(-\Sigma_t R_i) + F[Q(x_i),Q(x_{i-1}),\Sigma_t,R_i] \qquad (42)$$

for plane geometry,

$$I(r_i,\omega_p,E_j) = I(r',\omega',E_j)\exp(-\Sigma_t R_i) + F[Q(r_i),Q(r'),\Sigma_t,R_i] \qquad (43)$$

for spherical geometry.

Here

$$I(x_i,\omega_p,E_j) = E_j\Phi(x_i,\omega_p,E_j),$$

$$R_i = \left|\frac{x_i - x_{i-1}}{\omega_p}\right| \quad \text{for plane geometry} \tag{44}$$

$$= |r_i\omega_p - r'\omega'| \quad \text{for spherical geometry} \tag{45}$$

$F[\ ]$ = expression (40) or (41).

For $I(r',\omega')$ and $Q(r',\omega')$ in spherical geometry, in general a set of meshes (r',ω') is not coincident with a set of meshes (r_j,ω_q), which inevitably reguires interpolation for estimation of $I(r',\omega')$ and $Q(r',\omega')$. When $r'=r_{i\pm1}$ and $\omega_{p-1}<\omega_p<\omega_{p+1}$, both $I(\omega')$ and $Q(\omega')$ are obtained by applying a linear interpolation with respect to $\theta\equiv\cos^{-1}\omega$ in the current code (Fig.3A). While for $\omega'=\omega_{p\pm1}$ and $r_{i-1}<r'<r_{i+1}$, both $I(r')$ and $Q(r')$ are obtained by applying a linear interpolation with respect to r(Fig. 3B). The value for r' or θ' is determined referring to Fig.4 as follows:

i) For $0<\omega_p<1$ and $r'=r_{i-1}$,

$$\theta' = \sin^{-1}\left(\frac{r_i}{r_{i-1}}\sqrt{1-\omega_p^2}\right). \tag{46}$$

ii) For $0<\omega_p<1$ and $\omega'=\omega_{p+1}$,

$$r' = r_i\frac{\sqrt{1-\omega_p^2}}{\sqrt{1-\omega_{p+1}^2}}. \tag{47}$$

iii) For $-1<\omega_p<0$ and $r'=r_{i+1}$,

$$\theta' = \pi - \sin^{-1}\left(\frac{r_i}{r_{i+1}}\sqrt{1-\omega_p^2}\right). \tag{48}$$

iv) For $-1<\omega_p<0$ and $\omega'=\omega_{p+1}$,

$$r' = r_i\frac{\sqrt{1-\omega_p^2}}{\sqrt{1-\omega_{p+1}^2}}. \tag{49}$$

(3) New technique for treatment of the within-group scattering radiations instead of applying an iteration technique

Those radiations scattered within a certain small angle may be considered approximately as unscattered. PALLAS code calculates the within-group scattering radiations on the basis of this approximation: The radiations scattered within a certain small solid angle $\Delta\bar{\Omega}_p$ from their flight direction of $\bar{\Omega}_p$ are treated as unscattered. From simplicity in practical PALLAS calculations, this small solid angle is assumed to be constant for all the flight directional meshes assigned in advance. In the current PALLAS code it is assumed that $\Delta\bar{\Omega} = 2\pi\Delta\mu_l$ and $\Delta\mu_l = W_l$ for neutron, where W_l is the weight of μ_l in Gaussian quadrature, and $\Delta\mu_l = (\lambda_j - \lambda_{j-1})/4$ for gamma ray.

Consequently the scattered radiations to be treated as unscattered are calculated as

$$Q^N_{el}(x,\omega_p,E_j) = 2\pi W_l \Sigma_{el}(x,E_j) f(E_j,\mu_l) I(x,\omega_p,E_j) \tag{50}$$

for neutron,

$$Q^G(x,\omega_p,E_j) = 2\pi n(x) \frac{K(\lambda_j,\lambda_j)}{2\pi} I(x,\omega_p,E_j)\Delta\lambda_j \tag{51}$$

for gamma ray.

The radiations scattered inelastically within group are ignored because of general use of fine energy mesh intervals in MeV region.

Subtracting the expression (50) or (51) from the both hand sides of Eq.(1), we obtain the following equation with the notation of the energy flux for $\omega=\omega_p$ and $E=E_j$

$$\begin{aligned}\bar{\Omega}\nabla I + \Sigma_t(x,E_j)I(x,\omega_p,E_j) - A(x,E_j)I(x,\omega_p,E_j) \\ = \int\int dE' d\bar{\Omega}'(E_j/E') I(x,\omega',E') \Sigma_s(x,E'\to E_j,\bar{\Omega}'\to\bar{\Omega}_p) \\ - A(x,E_j)I(x,\omega_p,E_j) + S(x,\omega_p,E_j),\end{aligned} \tag{52}$$

where

$$A(x,E_j) = 2\pi W_l \Sigma_{el}(x,E_j) f(E_j,\mu_l) \tag{53}$$

for neutron,

$$= n(x) K(\lambda_j,\lambda_j) \Delta\lambda_j \tag{54}$$

for gamma ray.

The above equation (52) is rewritten in a form

$$\bar{\Omega}\nabla I + \Sigma_t' I = \int_{E>E_j} dE' \int_{\bar{\Omega}'\neq\bar{\Omega}_p} d\bar{\Omega}'(E_j/E) I \Sigma_s + S, \tag{55}$$

where

$$\Sigma_t'(x,E) = \Sigma_t(x,E) - A(x,E). \tag{56}$$

The final equation (55) can be rewritten as

$$I(x_i,\omega_p,E_j) = I(x_{i-1},\omega',E_j)\exp(-\Sigma_t' R_i) + F[Q'(x_{i-1}),Q'(x_i),\Sigma_t',R_i], \tag{57}$$

where

$$Q'(x) = Q_{el}'^{N} + Q_{in}^{N} + S \tag{58}$$

for neutron,

$$= Q'^{G} + S \tag{59}$$

for gamma ray,

and

$$Q_{el}'^{N} = \sum_{m=2}^{M} \sum_{n} W_m w_n \Sigma_{el}(x,E_{(m)}) f^m(E_{(m)}) I(x,\omega_n,E_{(m)}), \tag{60}$$

$$Q'^{G} = \sum_{k=1}^{j-1} \sum_{n} w_n n(x) \frac{K(\lambda_k,\lambda_j)}{2\pi} I(x,\omega_n,\lambda_k)\Delta\lambda_k. \tag{61}$$

Consequently the final expression for computer calculation is written instead of Eq. (42) or (43) as

$$I(x_i,\omega_p,E_j) = I(x_{i-1},\omega_p,E_j)\exp(-\Sigma_t' R_i) + F[Q'(x_i),Q'(x_{i-1}),\Sigma_t',R_i] \tag{62}$$

for plane geometry,

$$I(r_i,\omega_p,E_j) = I(r',\omega',E_j)\exp(-\Sigma_t' R_i) + F[Q'(r_i),Q'(r'),\Sigma_t',R_i] \tag{63}$$

for spherical geometry.

where Σ_t' is obtained from Exp.(56) and Q' from Exp.(58) for neutron or Exp.(59) for gamma ray.

(4) Secondary gamma-ray source produced by neutron reaction

Expressing the secondary gamma-ray source by $s(x,\omega,E_j^\gamma)$ at a gamma-ray energy mesh E_j^γ, we obtain the following expression:

$$s(x,\omega,E_j^\gamma) = \frac{1}{4\pi} \sum_k \Sigma_{n\gamma}(x,E_k^n \to E_j^\gamma)\Phi_0(x,E_k^n)\Delta E_k^n. \quad (64)$$

Here $\Sigma_{n\gamma}$ is the macroscopic neutron reaction cross section by which gamma rays of energy E_j^γ are produced per unit MeV by a neutron of energy E_k^n, and Φ_0 is the neutron scalar flux at energy E_k^n and ΔE_k^n its energy width.

(5) Annihilation gamma-ray source[5)]

The secondary gamma-ray source resulting from positron annihilation is calculated from

$$s(x,\omega,E_\ell^\gamma) = \sum_k \frac{2}{4\pi} \Sigma_{pp}(x,E_k^\gamma)\Phi_0(x,E_k^\gamma)\Delta E_k^\gamma. \quad (65)$$

The above expression is based on an assumption that the annihilation gamma rays are created at the point where the pair production reaction occurred and emitted isotropically. In the expression E_ℓ^γ=0.511 MeV and Σ_{pp} is the macroscopic pair production cross section.

(6) Bremsstrahlung photon source[5)]

First, we must evaluate the electrons produced from the main primary gamma-ray reactions such as Compton scattering, pair production and photoelectric effect. The Compton scattering electrons are calculated from the gamma-ray scattering source due to Compton scattering. Expressing the Compton scattering electron source by $s_e^c(x,\omega,E^e)$, we can obtain the following expression.

$$s_e^c(x,\omega,E^e) = \frac{1}{4\pi}\left[2\pi\int\frac{Q^G(x,\omega,\lambda)}{E^\gamma}d\omega\right]\delta(E^e-E^{\gamma'}+E^\gamma), \tag{66}$$

where E^e,$E^{\gamma'}$ and E^γ are respectively the energies of emergent electron, incident and emergent gamma rays, and $Q^G(x,\omega,\lambda)$ is the gamma-ray scattering source written in terms of energy flux, obtained from Eq.(32). The above expression is derived based on an assumption of isotropic emission of electrons for simplicity in practical calculation, although the moving direction of a recoil electron can be precisely determined from the formula of Compton scattering.

Pair production electrons and positrons are calculated based on an approximation that both electrons are emitted within a certain small solid angle around the direction of the primary gamma ray: The mean small emission angle θ_m can be approximated[7)] simply by

$$\theta_m = m_0c^2/E^{\gamma'}. \tag{67}$$

The energy spectrum of pair production electrons (also positrons) is determined based on the method of Bethe and Heitler[7)]. Consequently the pair produced electron source $s_e^p(x,\omega,E^e)$ is evaluated as

$$s_e^p(x,\omega,E^e) = \int_{2m_0c^2}^{E^\gamma_{max}} 2n(x)\sigma_{pp}(x,E^{\gamma'})f(E^{\gamma'}\to E^e) \times \int\Phi(x,\omega',E^{\gamma'})d\omega'dE^{\gamma'}, \tag{68}$$

where $\sigma_{pp}(x,E^{\gamma})$ is the microscopic pair production cross section and $f(E^{\gamma}\rightarrow E^{e})$ the probability distribution function, which is calculated from

$$f(E^{\gamma}\rightarrow E^{e}) = \frac{\sigma_{\gamma e}(E^{\gamma},E^{e})}{\int_{2m_0c^2}^{E^e_{max}} \sigma_{\gamma e}(E^{\gamma},E^{e})dE^{e}} \quad . \tag{69}$$

Further, E^{e}_{max} is the maximum kinetic energy transferred from the incident gamma-ray into pair produced electrons:

$$E^{e}_{max} = E^{\gamma'} - 2m_0c^2. \tag{70}$$

The above expression (68) can be numerically evaluated only if the matrix $f(E^{\gamma},E^{e})$ is known, which is written for a set of meshes (ω_p,E^{e}_{ℓ}) as

$$s^{p}_{e}(x,\omega_p,E^{e}_{\ell}) = 2n(x)\sum_{j=1}^{K}\sigma^{j}_{pp}f^{j,\ell}\Delta E^{\gamma}_{j}\sum_{q} w_q\Phi(x,\omega_q,E^{\gamma}_{j}), \tag{71}$$

where

$$E_K \geq 2m_0c^2$$

and for ω_q that satisfies the following relationship

$$1 \geq \omega_p - \cos\theta_j \geq \omega_q \geq \omega_p + \cos\theta_j \geq -1, \tag{72}$$

$$w_q = \Delta\omega_p/\Sigma_q\Delta\omega_q, \tag{73}$$

further

$$\theta_j = m_0c^2/E^{\gamma}_{j}. \tag{74}$$

The differential pair production cross section is calculated based on the Born approximation formalism[8];

$$\sigma_{\gamma e}(E^{\gamma},E^{e}) = \frac{Z^2r_0^2}{137}\cdot\frac{p_+p_-}{E^3}\left\{-\frac{4}{3} - 2E_+E_-\frac{p_+^2+p_-^2}{p_+^2p_-^2}\right.$$

$$\left. + (m_0c^2)^2\left(\frac{E_+\varepsilon_-}{p_-^3} + \frac{\varepsilon_+E_-}{p_+^3} - \frac{\varepsilon_+\varepsilon_-}{p_+p_-}\right)\right.$$

$$+ L\left[\frac{E^2}{p_+^3 p_-^3}(E_+^2E_-^2 + p_+^2p_-^2)\right.$$

$$- \frac{8}{3}\frac{E_+E_-}{p_+p_-} - \frac{(m_0c^2)^2E}{2p_+p_-}\left(\frac{E_+E_- - p_-^2}{p_-^3}\varepsilon_-\right.$$

$$\left.\left.+ \frac{E_+E_- - p_+^2}{p_+^3}\varepsilon_+ + \frac{2EE_+E_-}{p_+^2p_-^2}\right)\right]\}. \qquad (75)$$

In the above expression,

$E = E^\gamma/m_0c^2$ (gamma-ray energy in m_0c^2 units),

$E_+ = (E_+^e/m_0c^2)+1$ (total energy of positron in m_0c^2 units),

$E_- = (E_-^e/m_0c^2)+1$ (total energy of electron in m_0c^2 units),

$p_+ = [(E_+^e/m_0c^2)^2+2(E_+^e/m_0c^2)]^{1/2}$ (momentum of positron in m_0C units),

$p_- = [(E_-^e/m_0c^2)^2+2(E_-^e/m_0c^2)]^{1/2}$ (momentum of electron in m_0C units),

Z = atomic number of target material,

$r_0 = e^2/m_0c^2 = 2.82\times10^{-13}$ cm (classical electron radius),

$$\varepsilon_+ = 2\log\frac{E_+ + p_+}{m_0c^2},$$

$$\varepsilon_- = 2\log\frac{E_- + p_-}{m_0c^2},$$

$$L = 2\log\frac{E_+E_- + p_+p_- + (m_0c^2)^2}{m_0c^2E}.$$

Further, the gamma-ray angular flux $\Phi(x,\omega,E^\gamma)$ is directly obtained from the calculated energy flux:

$$\Phi(x,\omega,E^\gamma) = I(x,\omega,\lambda)/E^\gamma. \qquad (76)$$

Finally, the electrons produced by the photoelectric effect are calculated based on an assumption of isotropic emission of electrons:

$$s_e^{Ph}(x,\omega,E^e) = \frac{1}{4\pi}\int_{4\pi} n(x)\sigma_{Ph}(x,E^\gamma)\phi(x,\omega,E^\gamma) \times \delta(E^e-E^\gamma+E_{BK})\,d\bar{\Omega}, \quad (77)$$

where $\sigma_{Ph}(x,E^\gamma)$ is the photoelectric effect cross section and E_{BK} the binding energy of K-shell electrons. The binding energies of the other shells are ignored.

From the above calculations, the total electron source $s_e(x,\omega,E^e)$ is obtained by summing the three electron sources as

$$s_e(x,\omega,E^e) = s_e^c(x,\omega,E^e) + s_e^p(x,\omega,E^e) + s_e^{Ph}(x,\omega,E^e). \quad (78)$$

The electron energy slowing down calculation can be made using the continuous slowing down model, since it may be assumed that the bremsstrahlung photons produced by primary gamma rays below 10 MeV originate at the spatial mesh point where the primary gamma-ray interaction occured. Consequently the electron angular flux $\phi(x,\omega,E^e)$ is calculated using the electron stopping power $St(E^e)$ as

$$\phi(x,\omega,E^e) = \frac{\int_{E^e}^{E^e_{max}} s_e(x,\omega,E^e)\,dE^{e'}}{St(E^e)}, \quad (79)$$

where E^e_{max} is the maximum energy of electrons produced from the three primary gamma-ray interactions.

In general the bremsstrahlung photons produced from a high energy electron are emitted within small angular cone around the direction of electron motion, however, its emission angle becomes wide with decreasing the electron energy. Then we adopt the same simplified approximation for the emission angle as in the pair produced electrons:

$$\theta_m = m_0c^2/(E^e + m_0c^2). \quad (80)$$

The bremsstrahlung photon source is calculated from

$$s_\gamma(x,\omega,E^\gamma) = \int_{E^\gamma}^{E^e_{max}} N(x)\sigma_B(E^e\to E^\gamma)\phi(x,\omega,E^e)dE^e$$

$$= \int_{E^\gamma}^{E^e_{max}} N(x)\sigma_B(E^e\to E^\gamma)\frac{\int_{E^e}^{E^e_{max}} s_e(x,\omega,E^{e'})dE^{e'}}{St(E^e)} \times dE^e, \quad (81)$$

where $N(x)$ is the number density of target material and $\sigma_B(E^e\to E^\gamma)$ the bremsstrahlung production cross section, which is calculated with EELOSS code[9] implemented as one of subroutines in PALLAS-PL,SP-Br code. The data for this cross section are calculated based on Koch and Motz[10] and Berger and Seltzer[11]. The calculational equations for obtaining the cross section data are given in Ref.(9). The above expression (81) is numerically evaluated for a set of meshes (ω_p, E^γ_j) as

$$s_\gamma(x,\omega_p,E^\gamma_j) = \sum_{\ell=1}^{L} N(x)\sigma_B^{\ell,j}\Delta E^e_\ell \times \frac{\sum_{m=1}^{\ell}\sum_q w_q\, s_e(x,\omega_q,E^e_m)\Delta E^e_m}{St(E^e_\ell)}, \quad (82)$$

where for ω_q that satisfies the relationship of

$$1 \geq \omega_p - \cos\theta_m \geq \omega_q \geq \omega_p + \cos\theta_m \geq -1, \quad (83)$$

$$w_q = \Delta\omega_p/\sum_q\Delta\omega_q, \quad (84)$$

and

$$\sigma_B^{\ell,j} = \sigma_B(E^e_\ell\to E^\gamma_j),$$

$$\theta_m = m_0c^2/(E^e_m + m_0c^2).$$

Since the bremsstrahlung photon source is numerically evaluated by Eq.(82), then this source is used for executing the secondary gamma-ray transport calculation using PALLAS-PL,

SP-Br code again.

(7) Slowing down calculation into thermal group and convergence

Slowing down calculation from higher energies into thermal group is carried out through two ways: The first is that due to scattering by hydrogen, which is numerically evaluated based on an assumption of isotropic scattering for producing of no appreciable error in practical calculations, given by

$$Q^{h}(x,\omega,E_{th})\Delta E_{th} = \sum_{k=1}^{JJ-1} \frac{\Sigma_{el}(E_k)\Phi_0(x,E_k)\Delta E_k \Delta E_{th}}{4\pi E_k} , \qquad (85)$$

where

$$\Phi_0(x,E_k) = 2\pi\int\Phi(x,\omega,E_k)d\omega,$$

and

$$\Delta E_{th} = E_{th}^{u} - 0 \cong E_{th}\ (1 + 0.5\Delta u), \qquad (86)$$

further Δu is the lethargy width.

On the other hand, the other is that due to scattering by all nuclides other than hydrogen, which is numerically evaluated based on again an assumption of isotropic elastic scattering and of disregarding inelastic scattering component for producing negligible error in practical calculations, give by

$$Q(x,\omega,E_{th})\Delta E_{th} = \frac{\Sigma_{el}(E_{JJ-1})\Phi_0(x,E_{JJ-1})\Delta E_{JJ-1}}{4\pi\frac{\Delta u}{\xi}} , \qquad (87)$$

where ξ is the average logarithmic energy decrement per collision given by

$$\xi = 1 + \frac{(A-1)^2}{2A} \ln\frac{A-1}{A+1} . \qquad (88)$$

The iterative thermal group calculations are continued until the scalar flux converges according to a criterion:

$$\text{Max}\ \left[\left|\frac{\Phi_0^n(x)-\Phi_0^{n-1}(x)}{\Phi_0^n(x)}\right|\right] < \text{EPSRN} \tag{89}$$

for all spatial meshes.

(8) Mono-energy source calculation

Since the original PALLAS calculation is made fundamentally based on a continuous energy source, it can not treat a mono-energy source problem. For mono-energy source calculations, special routines have been added to the original PALLAS code. In gamma-ray transport calculation the special routine is contained in a subroutine HIMEJI dealing with gamma-ray scattering calculation. The gamma-ray mono-energy source calculation is made as follows: First, the uncollided flux is calculated and printed as output, then the scattered source is calculated based on Eq.(31) as

$$Q(x,\omega,E_0) = n(x)\frac{3}{4}\mu_T I^{(u)}(x,\omega,E_0)\lambda_0\frac{\Delta E_0}{E_0}, \tag{90}$$

where E_0 is the incident source energy and $I^{(u)}$ the unscattered energy flux. Consequently the scattered energy flux at $E=E_0$ is calculated using the source $Q(x,\omega,E_0)$ in the PALLAS code. The analytical solution for the scattered flux $I^{(s)}$ is obtained for monodirectional incidence on a plane shield as follows:

$$\omega_0\frac{dI^{(s)}}{dx} + \mu I^{(s)} = \frac{n(x)}{2\pi}\frac{3}{4}\mu_T\frac{E_0}{\omega_0}e^{-\frac{\mu x}{\omega_0}}\frac{\lambda_0}{E_0}$$

$$= \frac{n(x)}{2\pi}\frac{3}{4}\mu_T\frac{\lambda_0}{\omega_0}e^{-\frac{\mu x}{\omega_0}}. \tag{91}$$

The solution of the above equation is

$$I^{(s)}(x,\omega_0,E_0) = \frac{1}{2\pi\omega_0} e^{-\frac{\mu x}{\omega_0}} \int_0^x e^{\frac{\mu t}{\omega_0}} a\, e^{-\frac{\mu t}{\omega_0}} dt$$

$$= \frac{1}{2\pi\omega_0} a\, x\, e^{-\frac{\mu x}{\omega_0}}$$

$$= n(x)\frac{3}{4}\mu_T \frac{\lambda_0 x}{2\pi\omega_0^2} e^{-\frac{\mu x}{\omega_0}} . \qquad (92)$$

For a perpendicular incidence $\omega_0=1$

$$I^{(s)}(x,\omega_0,E_0) = \frac{n(x)}{2\pi}\cdot\frac{3}{4}\mu_T \frac{\lambda_0}{\mu}(\mu x)e^{-\mu x}, \qquad (93)$$

and

$$I_0^{(s)}(x,E_0) = n(x)\frac{3}{4}\mu_T \frac{\lambda_0}{\mu}(\mu x)e^{-\mu x}. \qquad (94)$$

While for a plane isotropic incidence

$$Q(x,\omega,E_0) = \frac{n(x)}{4\pi\omega}\cdot\frac{3}{4}\mu_T\lambda_0 e^{-\frac{\mu x}{\omega}}, \qquad (95)$$

hence

$$I^{(s)}(x,\omega,E_0) = n(x)\frac{3}{4}\mu_T\lambda_0 \frac{x}{2\pi\omega^2} e^{-\frac{\mu x}{\omega}}, \qquad (96)$$

and

$$I_0^{(s)}(x,E_0) = n(x)\frac{3}{4}\mu_T\lambda_0\cdot 2\pi\int_0^1 \frac{x}{2\pi\omega^2} e^{-\frac{\mu x}{\omega}} d\omega$$

$$= a\cdot\int_{-\infty}^{-\mu x} \frac{x}{\omega^2}\left(\frac{\omega^2}{\mu x}\right) e^t dt$$

$$= n(x)\frac{3}{4}\mu_T \frac{\lambda_0}{\mu} e^{-\mu x}. \qquad (97)$$

The above expressions (94) and (97) are used to check PALLAS calculation. For a point isotropic source the following expression is used for this purpose:

$$I_0^{(s)}(r,E_0) = n(x)\frac{3}{4}\mu_T \frac{\lambda_0}{\mu} \frac{\mu x}{4\pi r^2} e^{-\mu x}. \tag{98}$$

For energies other than the source energy,

$$Q(x,\omega,\lambda_j) = \int_0^{\pi} n(x)\frac{K(\lambda_0,\lambda_j)}{\pi}\cdot\frac{\lambda_0}{E_0} I^{(u)}(x,\omega',\lambda_0)d\psi, \tag{99}$$

the above scattering source is used for calculation of the angular flux in PALLAS calculation except for a plane perpendicular incidence ω_0=1.0 and a point isotropic source. For these cases the single scattered source shows still a δ-function distribution, consequently the source is given by

$$Q(x,\omega,\lambda_j) = n(x)K(\lambda_0,\lambda_j)\frac{\lambda_0}{E_0} I^{(u)}(x,\omega_0,\lambda_0)\times \delta(\omega-1-\lambda_0+\lambda_j). \tag{100}$$

On the other hand for neutron transport calculation the special routine HAMATU executes the mono-energy source calculation. In contrast to gamma-ray scattering neutron never degrades considerably its energy except for hydrogen. To evaluate neutron fluxes at the source and next energy meshes as accurately as possible, the energy region around the source energy is devided into fine energy meshes illustrated in Fig.5. At the fine meshes the mono-energy neutron source is defined as drawn by the step function in the figure: The weights for the source intensity are defined as 1.0, 2.0, 3.0, 3.0, 2.0 and 1.0 at the finely divided energy meshes $e_{1\sim6}$. The source normalization is made as

$$\begin{aligned} S.N. &= \frac{SNORM}{\sum_{n=1}^{6} s_n \Delta e_n} \\ &= \frac{SNORM}{20E_0\Delta u}, \end{aligned} \tag{101}$$

where SNORM is the source intensity defined by an input, and E_0 and Δu are respectively the source energy and lethargy width. The neutron transport calculation is carried out at the fine energy meshes from e_1 through e_6 for thus defined continuous

energy source and is continued at the meshes from e_9 through e_{12}. Since e_{12} is equal to E_2 energy mesh, the next transport calculation starts at E_3 energy mesh. Usually one-dimensional neutron calculation is made with a lethargy with of 0.1 for high energy region, which means that the finely divided energy mesh interval becomes 0.1/8=0.0125 lethargy.

4. Restriction of Input Data

The present PALLAS-PL,SP-Br code is written by fixed dimension. The main restriction of input data is as follows:

(1) Total energy meshes JJ $\leq$ 120
(2) Total spatial meshes MRR $\leq$ 150
(3) Total material regions II $\leq$ 20
(4) Total nuclides NUCT $\leq$ 30
    (Nuclides other than hydrogen $\leq$ 20)
(5) Total angular meshes IQ $\leq$ 30
    (IQ = 16 or 20 or 28 quadrature set is defined in Block Data.)
(6) Total number of responses $\leq$ 20

5. Program Structure

The structure map of PALLAS-PL,SP-Br program is shown in Fig.6, in which the main routine defining only variable dimensions SEL(m_1, m_2, m_3) and PPA(n_1, n_2, 20) is omitted for simplicity. All the subroutines used in the program are listed in Table 1 together with short comments.

4. Restriction of Input Data

The present PALLAS-PL,SP-Br code is written by fixed dimension. The main restriction of input data is as follows:

(1) Total energy meshes JJ $\leq$ 120
(2) Total spatial meshes MRR $\leq$ 150
(3) Total material regions II $\leq$ 20
(4) Total nuclides NUCT $\leq$ 30
    (Nuclides other than hydrogen $\leq$ 20)
(5) Total angular meshes IQ $\leq$ 30
    (IQ = 16 or 20 or 28 quadrature set is defined in Block Data.)
(6) Total number of responses $\leq$ 20

5. Program Structure

The structure map of PALLAS-PL,SP-Br program is shown in Fig.6, in which the main routine defining only variable dimensions SEL(m_1, m_2, m_3) and PPA(n_1, n_2, 20) is omitted for simplicity. All the subroutines used in the program are listed in Table 1 together with short comments.

6. Informations for Users

6.1 Input Specification

Card 1 MMX, MIQ, MJJ (3I3)

MMX=0, no bremsstrahlung photon transport calculation.
=number of total spatial meshes.

MIQ=0, no brems. transport cal.
=number of angular meshes.

MJJ=0, no brems. transport cal.
=number of energy meshes.

These variable parameters are used to define the dimensions of the secondary photon source SEL(MMX, MIQ, MJJ) and also the pair production energy distribution PPA(MJJ, MJJ, 20 (regions)). Without bremsstrahlung transport calculation these dimensions are defined as SEL(1,1,1) and PPA(1,1,20).

Card 2 Title card PROBLEM (20A4)

Card 3 Control Integers for a Problem

KNDG, KIN, NORF, KTST (4I3)

KNDG=1, only neutron calculation.
=2, neutron-secondary gamma-ray calculation.
=4, only gamma-ray calculation.

KIN=0, no effect.
=1 or 2, series calculation for neutron (Data note 1).

NORF=0, no effect.
>0, no reflection at the left boundary in plane geometry.

KTST=0, no effect.
=-1, check of input data read in and no transport calculation.

Card 4 NGEOM, MONOE, MNODRE, IBREM, IPRNT (5I3)

NGEOM=1, plane geometry.
=2, spherical geometry.

MONOE=0, continuous energy source.
=10, mono-energy problem.

MNODRE=1, plane perpendicular incidence or point isotropic source.
=n<20, plane slant incidence at n-th angular mesh.
≥20, plane isotropic incidence.

IBREM=0, no bremsstrahlung photon transport calculation.
=1, bremsstrahlung photon transport calculation.

IPRNT=0, print only input data and calculated scalar flux at each energy mesh and reaction rates (dose rate etc).
=1, print also angular fluxes at each energy mesh.
=2, print also detailed constants such as pair production energy distribution, differential elastic scattering cross section, inelastic scattering matrix and bremsstrahlung photon production cross section.

Card 5 JN(N), N=1, KIN+1 (4I3)

JN(N)=number of energy meshes at N-th calculation in the neutron series calculation (KNDG≤2). For gamma-ray calculation (KNDG=4) the number of energy meshes at N=1. (Data note 2)

Card 6 II, IQ, IFIS, JSTAT (4I3)

II=number of material regions.

IQ=number of angular meshes.

IFIS=0, source energy spectrum S(E) is read in from cards.
=1, fission spectrum is computed in the program. Do not enter S(E).
$S(E)=0.484 \sinh \sqrt{2E} \cdot e^{-E}$ for neutron,
=14.0 exp (-1.10E) for photon.

JSTAT=0, calculation starts at first energy mesh.
=n, calculation starts at n-th energy mesh. Flux calculation up to (n-1)-th energy mesh is omitted.

Card 7 NBND, MSR, IQIQ, JDTAL (4I3)

NBND=0, volume source problem.

=10, boundary flux problem.

MSR=0, for NBND=10.

=n, source spatial distribution is inputed up to n-th mesh.

IQIQ=0, fixed angular quadratures are used: IQ=16, 20 and 28.

=n≤30, angular quadrature set is inputed.

JDTAL=0, no effect.

=4, neutron calculation in detailed energy mesh intervals between several MeV and 0.2 MeV (Data note 3).

Card 8 EMAX, HH, SNORM, RDST (4E10.3)

EMAX=maximum energy in MeV.

HH=0.0 for gamma-ray calculation (additional Data note).

=0.1 or 0.2 or 0.4, lethargy interval for neutron calculation.

SNORM=source normalization.

RDST=radial distance in cm at the first radial mesh at which the boundary flux is defined for NBND=10.

=0.0, otherwise.

If IQIQ>0, Card 9 and 10 are inputed.

Card 9 (WP(N), N=1, IQ) (8E10.3)

Angular quadrature.

Card 10 (WWP(N), N=1, IQ) (8E10.3)

Angular quadrature weight.

Card 11 MES(n), n=1, II (20I3)

Number of meshes in n-th material region.

Card 12 RR(n), n=1, II (8E10.3)

Thickness in cm in n-th material region.

If KNDG=4, Card 13 is inputed.

Card 13 E(j), j=1, JJ (8E10.3)

Energy (MeV) at j-th energy mesh for gamma-ray calculation.

Do not enter them for KNDG=2, because secondary gamma-ray

energy mesh points are fixed. If HH>0, do not enter them.

Card 14 SE2(j,k), j=1, JN(k) (8E10.3)

for k=1, ---, KIN+1

Source energy distribution (n/MeV) at j-th energy mesh of k-th energy mesh block. For KNDG=4, energy distribution for gamma ray is given in SE2(j,1). Do not enter them if IFIS=1, or if MONOE>0.

If NBND=0, Card 15-1 is inputed.

Card 15 SR(n), n=1, MSR (8E10.3)

Source spatial distribution ($n/cm^3 \cdot sec$) at n-th spatial mesh point. Then the volume source is expressed by

$$S(x,E) = SR(x)*SE2(E_j)\ n/cm^3 \cdot sec \cdot MeV.$$

For NBND=10, the boundary angular flux is defined in terms of $n/cm^2 \cdot sec \cdot sr \cdot MeV$ by

$$BOUND(\omega_n, E_j) = BD2(\omega_n, E_j)*SE(E_j).$$

Card 15-2 BD2(n,j,k), n=1, IPQK (8E10.3)

for j=1, 2, ---, JN(k) at k=1, ---, KIN+1

Boundary angular flux ($n/cm^2 \cdot sec \cdot sr$) at $\omega_n>0$ at j-th energy mesh of k-th energy mesh block. For only MONOE=0 and NGEOM=1 or MONOE=0, NGEOM=2 and MNODRE≠1, Card 15-2 is read.

For a point isotropic continuous energy (such as the fission spectrum) source, one should specify NGEOM=2, MONOE=0, MNODRE=1, (IFIS=1) and NBND=10. Then the boundary angular flux is defined by

$$BD2(1,j,k) = \frac{SNORM}{4\pi \cdot RDST**2(2\pi WWP(1))}.$$

If NBND=10, MONOE>0 and MNODRE=0, Card 15-3 is inputed.

Card 15-3 BOUND(n,1), n=1, IPQK (8E10.3)

Boundary angular flux at the source energy.

For a point isotropic monoenergy source, one should specify NGEOM=2, MONOE=10, MNODRE=1 and NBND=10. Then the boundary angular flux is defined by

$$\text{BOUND}(1,1) = \frac{\text{SNORM}}{4\pi \cdot \text{RDST}**2\,(2\pi \text{WWP}(1))} .$$

For a monoenergy monodirectional incidence, one should specify NGEOM=1, MONOE=10, MNODRE=n and NBND=10. Then the boundary angular flux is defined by

$$\text{BOUND}(n,1) = \frac{\text{SNORM}}{2\pi \cdot \text{WP}(n) \cdot \text{WWP}(n)} .$$

For a monoenergy isotropic incidence, one should specify NGEOM=1, MONOE=10, MNODRE=20 and NBND=10. Then the boundary angular flux is defined by

$$\text{BOUND}(n,1) = \frac{\text{SNORM}}{2\pi \cdot \text{WP}(n)}$$

for all n in WP(n)>0.

For neutron thermal group calculation in KNDG=1 or 2, Card 16 and 17 are inputed.

Card 16 LTAL, LUT (2I3)

LTAL=10, thermal group calculation.

LUT=n, termination of iterative group calculation.

Card 17 ESRN (E10.3)

Convergence criterion.

Do not enter them unless KIN>0.

Card 18 NOEL(i), i=1, II (20I3)

Number of nuclides inputed in i-th material region (Data note 4). Maximum number of nuclides in all the regions is 21. If KNDG=4, do not enter them.

Card 19 NEK(i), i=1, II (20I3)

Identification numbers of material regions (Data note 5). If KNDG=4 and II=1, do not enter them.

The input data described below are those for nuclear data read in repeatedly every material.

For neutron data (KNDG=1 or 2),

Card 20 MATERIAL (8A4)

Name of material.

Card 21 NUCLID (8A4)

Symbol of nuclide.

Card 22 MATN, AMAS, AN, ICH (I5, 2E10.5, I5)

MATN=identification number of nuclide (4 digits given in Table 2).

AMAS=atomic mass.

AN=atomic density ($\times 10^{24}$).

ICH=0, no effect.

>0, $\sigma_t(E_j)$ and $\sigma_{el}(E_j)$ are read in from cards, by which the cross sections of total and elastic scattering read in from the PALLAS library are replaced.

For ICH>0,

Card 23 SIGT(j), j=1, JJ (8E10.3)

$\sigma_t(E_j)$, microscopic total cross section at energy E_j (barn).

Card 24 SIGMA(j), j=1, JJ (8E10.3)

$\sigma_{el}(E_j)$, microscopic elastic scattering cross section at E_j (barn).

For gamma ray data (KNDG=4),

Card 20 MAT, MATERIAL (I3, 8A4)

MAT=identification number of material (last 3 digits given in Table 2, for instance 820 for lead).

Card 21 AN, ZN, BNUCD, DENS, BNEY (5E10.3)

AN=electron density in a materal ($\times 10^{24}$).

ZN=atomic number of a material.

BNUCD=atomic density in a material ($\times 10^{24}$).

DENS=material density (g/cm^3).

BNEY=binding energy of the K-shell electron (MeV).

For only a primary gamma-ray calculation, ZN=0.0, BNUCD=0.0, BNEY=0.0. When one calculates a bremsstrahlung photon transport, one should specify the data for ZN, BNUCD, DENS and BNEY.

Input data for specifying external data and output.

Card-01 ITP21, ITP22, ITP23 (3I3)

ITP21=0, no effect.

>0, calculated angular fluxes are stored in Tape 21.

ITP22=0, no effect.

>0, calculated scalar fluxes are stored in Tape 22.

ITP23=0, no effect.

>0, calculated reaction rates are stored in Tape 23.

Card-02 MRK, MRKK, IDOS, IEF, ICUR (5I3)

MRK=n, number of spatial meshes at which scalar fluxes (and angular fluxes if IPRNT=1) are printed.

MRKK=0, no effect.

=1, print $4\pi r_i^2 \exp(\mu r_i)*I(r_i,E_j)$ for a point isotropic source, or $\exp(\mu x_i)*I(x_i,E_j)$

for a plane monodirectional or isotropic incidence ($i=1,2,---,n$).

IDOS=0, print dose rates in units of mrem/h.

=n, print number of n reaction rates such as $^{27}Al(n,\alpha)$, $^{58}Ni(n,p)$ and $^{127}Au(n,\gamma)$.

For KNDG=4, in addition to dose rates in mrem/h dose rates in mr/h, absorption in erg/g using energy transfer coefficient and erg/g using energy absorption coefficient are also printed.

IEF=0, scalar fluxes are printed.

=1, energy fluxes are printed ($E*n/cm^2 \cdot sec \cdot (sr) \cdot MeV$).

ICUR=0, no effect.

>0, currents are printed ($\sum_p \omega_p \Phi_0(x_i,E_j)\Delta\omega_p$ or $\sum_p \omega_p I_0(x_i,E_j)\Delta\omega_p$).

If MRK>0, Card-03 is inputed.

Card-03 KR(n), n=1, MRK (20I3)

Spatial mesh numbers at which fluxes are printed if MRK>0.

If MRKK>0, Card-04 is inputed.

Card-04 RMU(n), n=1, MRK (8E10.3)

$\mu_i r_i$ or $\mu_i x_i$ in mfp ($i=1,2,---,n$).

If IDOS>0, Card-05 and 06 are inputed.

Card-05 REACTN (12A4)

Name of reaction rates.

Card-06 RESP(j,n), j=1, JJ (8E10.3)

for n=1,2,---,IREAC.

Response functions for calculating reaction rates.

6.2 Detailed Data Notes

(1) Data note 1

The PALLAS neutron transport calculations (KNDG=1 or 2) are made based on the nuclear data from the PALLAS neutron library, in which the energy mesh structures are defined by constant lethargy widths such as 0.05, 0.1, 0.2 and 0.4 as shown in Table 2. In general the structure of 0.1 lethargy width is used for fast neutron transport calculations above several hundred KeV, and that of 0.2 lethargy width is used for neutron calculations in intermediate energy region between several KeV and several hundred KeV, and for lower energy region the structure of 0.4 lethargy width is used. Consequently the neutron transport calculation is made using all the structures of 0.1, 0.2 and 0.4 lethargy widths. In this case these structures are used in a series as illustrated in Fig.7 as an example. In this figure the fast neutron transport calculation is made with 39 energy meshes of the 0.1 lethargy-width structure, then after computation the calculated fast neutron angular fluxes are transferred to those at the first 20 energy meshes of the next 0.2 lethargy-width calculation and the intermediate neutron transport calculation with 43 energy meshes starts at 21 energy mesh. After computation the calculated angular fluxes are again transferred to those at the first 22 energy meshes of the 0.4 lethargy-width calculation and the lower-energy neutron transport calculation with 45 energy meshes starts at 23 energy mesh.

When one uses the series calculation of lethargy-width structures, one should input an integer of 1 or 2 into KIN in Card 3: In the case of KIN=2, the structures of 0.1+0.2+0.4 or 0.05+0.1+0.2 lethargy widths are used, while in the case of KIN= 1, the sturctures of 0.1+0.2 or 0.05+0.1 lethargy widths are used. For KIN=0, only one structure of 0.05 or 0.1 lethargy width is used. For gamma-ray calculations always KIN=0(KNDG=4).

(2) Data note 2

In the neutron series calculation described in Data note 1, the total energy meshes JJ must be specified for the three lethargy-width transport calculations such as 0.1, 0.2 and 0.4 lethargy-width structures for KIN=2. For the example shown in Fig.7, JN(1)=39, JN(2)=43 and JN(3)=45. If KIN=1, JN(1)=n and JN(2)=m.

(3) Data note 3

The neutron spectrum becomes to show abrupt increase in the energy region between several MeV and several hundred KeV with increasing penetration distances into heavy materials such as iron and lead. PALLAS calculation with the 0.1 lethargy-width sturcture, however, underestimates the energy spectrum in this energy region at penetration distances beyond about 30 cm in an iron shield. This is attributable to the use of rather rough lethargy interval compared with that of maximum neutron slowing down in a single elastic scattering. Then the 0.1 lethargy interval can be divided equally into four sub-intervals. If one wants to use the detailed energy mesh calculation, one should specify 4 for JDTAL.

(4) Data note 4

One of characteristics in the method used in PALLAS code is to deal with as precisely as possible the neutron scattering calculation. For this purpose PALLAS executes the neutron scattering calculation for each nuclide. Then one must specify the number of nuclides in each material region. It is ideal that all the nuclides included in each material are specified, however, this is not realistic from the view point of computation time. One of practical ways is to choose only main nuclides that contribute considerably to neutron reaction. In this case for conservation of total atomic densities in a material the atomic densities of the rest nuclides must be added to those of the chosen main nuclides.

One should note that the number 0 is specified to a void region, so that no nuclear data are read in and no scattering calculation is required. This is effective in particular for radiation streaming calculations.

(5) Data note 5

All the material regions are numbered as illustrated in Fig.8. Fundamentally at first the numbers 1, 2, ---, $n \leq 20$ are set for respectively 1, 2, ---, n regions. When the same materials are repeatedly specified in material regions, their identification numbers are replaced by those of the previous defined same materials as shown in the figure. One should note that the number 0 is specified to a void region as described in Data 4.

(6) Additional Data note

Originally, the energy meshes for gamma-ray calculation are always defined by inputed data. Later the program has been modified so that these values can be defined automatically in it. For this purpose one should define only ΔE by the input HH in units of MeV. Here ΔE is the energy mesh difference with a same energy interval in high energy region (closer to a maximum gamma-ray energy EMAX). This energy-mesh structure, however, is not appropriate for PALLAS gamma-ray calculation, since the wavelength interval defined by the energy mesh interval ΔE becomes too large to calculate accurate gamma-ray transport. For instance, in the case of EMAX=1 MeV and HH=0.1 MeV, the first four wavelength intervals $\Delta\lambda_j$ (j=1,2,3,4) are less than 0.1, however for lower energy meshes such as 0.4, 0.3, and 0.2 MeV these intervals become considerably large such as 0.43 and 0.85. To mitigate such an abrupt increase in wavelength interval the code provides a special definition for the wavelength interval: At first the wavelength interval determined from ΔE is fairly small compared with a value of 0.1, however soon it exceeds the value of 0.1, at which the code

redefines 0.1 for the wavelength interval and after that its values are given by

$$\Delta\lambda_j = \Delta\lambda_{j-1} \times 1.3$$

for $\Delta\lambda_j \leq 0.5$ and $E_j > 0.06$ MeV,

or for $\Delta\lambda_j \leq 0.7$ and $E_j < 0.06$ MeV.

Example for 1 MeV and HH=0.1 MeV

No.	E_j	λ_j	$\Delta\lambda_j$
1	1.00	0.511	
2	0.90	0.568	0.058
3	0.80	0.639	0.071
4	0.70	0.730	0.091
5	0.616	0.830	0.100
6	0.532	0.960	0.130
7	0.453	1.129	0.169
8	0.379	1.349	0.220
9	0.313	1.635	0.286
10	0.255	2.007	0.372
11	0.205	2.491	0.484
12	0.171	2.991	0.500
13	0.146	3.491	0.500
14	0.128	3.991	0.500
15	0.114	4.491	0.500
16	0.102	4.991	0.500
17	0.093	5.491	0.500
18	0.085	5.991	0.500
19	0.079	6.491	0.500
20	0.073	6.991	0.500
21	0.068	7.491	0.500
22	0.066	7.791	0.500
23	0.060	8.491	0.700
24	0.056	9.191	0.700
25	0.052	9.891	0.700
26	0.048	10.591	0.700
27	0.045	11.291	

6.3 Special Notes

(1) Spatial mesh assignment

An equal spatial mesh interval is assigned in each material region as illustrated in Fig.9. In Fig.9(A) an example of the mesh assignment is shown for the case of plane geometry, in which two meshes are assigned at every inner boundary. In Fig.9(B) it is shown for the case of a volume source problem (NBND=0) in spherical geometry, in which no radial mesh is assigned at r=0 cm. On the other hand for the case of a boundary flux problem (NBND=10) in spherical geometry, it is illustrated in Fig.9(B-2), in which the boundary angular flux is defined at r=RDST cm.

(2) Secondary gamma-ray energy structure fixed in the code

Since the secondary gamma-ray transport calculation should be made based on the nuclear data on γ production cross section included in the PALLAS neutron library, the gamma-ray energy meshes must be in advance defined. Table 4 gives the gamma-ray energies defined and used in the library. The gamma-ray production cross sections from neutron energy points E_k^n(k=1, 2, ---) to gamma-ray energy points E_j^γ(j=1, 2, ---, 25) are given for each neutron lethargy-width structure in the library.

(3) Angular quadrature sets

Three angular quadrature sets are prepared in PALLAS-PL,SP-Br code. Two are Gaussian quadratures of 16 and 20 points, the other is an asymmetrical quadrature of 28 points, which are given in Table 5. The asymmetrical 28-point quadrature is suitable for detailed transport calculations of a point isotropic gamma-ray source problem. If one wants to use one of these fixed quadratures, one may specify only IQ=16 or 20 or 28 and IQIQ=0.

(4) PALLAS neutron library

Infinite dilution point energy data have been prepared in PALLAS neutron INF library, in which the microscopic total, capture and elastic scattering cross sections, σ_t, σ_c and σ_{el}, were averaged over the energy intervals defined as UPPER BOUND and LOWER BOUND for the energy meshes in each lethargy-width structure shown in Table 3. The averaging the nuclear data taken from ENDF/B-IV data library was made through the use of NJOY data processing code system[12]. The weighting functions used are the fission spectrum and 1/E spectrum. All the Legendre polynomial expansion coefficients given in ENDF/B-IV were used for making the scattering distribution functions $f_{el}(E_j,\mu)$ at all the neutron energies given in ENDF/B-IV file. Table 6 provides the orders of Legendre expansion and the lower bounds of neutron energy down to which the Legendre data are given. Both inelastic scattering matrix and secondary gamma-ray production cross section are also generated through NJOY code system. More detailed information on the PALLAS infinite dilution data is given in Ref.(13).

Effective cross section data have been prepared in PALLAS neutron EFF library. These effective cross sections were generated through RIFF code[14]. Detailed information is also given in Ref.(13).

Note that only EFF library contains the nuclear data for the materials, SUS(304), SUS(316), Ordinary and Heavy concretes. Further, if one uses Ordinary or Heavy concrete as an input material, one must specify two nuclides: the one is hydrogen with its atomic density and the other is Ordinary or Heavy concrete with its atomic density of 1.0. Because the effective cross sections for these concretes were generated by excluding only hydrogen from their atomic compositions. The reason why such a hydrogen exclusion was made is that the PALLAS code separates hydrogen from non-hydrogeneous nuclides in the neutron

scattering calculation for the purpose of accurate neutron scattering treatment. When one uses SUS(304) or SUS(316), one may specify its atomic density of 1.0.

(5) PALLAS gamma-ray library

The data for gamma-ray total, pair production and photoelectric effect cross sections have been taken from Hubbell's compilation[15]. Since these data were given only at certain defined energy points, the data used in PALLAS calculations are determined by interpolating linearly between these defined energy points. The identification numbers of nuclides or materials shown in Table 2 are utilized again in the gamma-ray library, however, only lower three figures in the four figures are valid because of no constraint of lethargy interval.

When one wants to calculate gamma-ray transport with KNDG= 4, one may specify only three figures in the four figures given in Table 2. In addition to stainless steel and concrete, water and air have been also included in the gamma-ray library. Their identification numbers are :

Water, 540
Air, 550.

The PALLAS gamma-ray library contains the data of energy flux to dose equivalent rate conversion factor (mrem/h), energy flux to exposure dose rate conversion factor (mr/h), and mass energy transfer and mass energy absorption coefficients to calculate the absorbed dose (erg/g) from energy flux. These data have been taken from Ref.15), 16) and storm's data[17]. Note that the data on energy flux to dose equivalent rate conversion factor from Ref.16) differ considerably around 0.1 MeV from old data[18].

6.4 External and Internal Data Files

All the files used for input, output, PALLAS libraries, storing calculated data and scratch data are give in Table 7.

6.5 Main Program Variables and Program Mnemonics

Relation of main variables used in the PALLAS program to program mnemonics is given in Table 8.

6.6 Sample Problems

(1) Sample problem 1: Gamma-ray plane isotropic incidence on lead

The input data for this problem are shown in Fig.10, in which the numbers 1 through 16 in both sides represent those of the input data cards. The first three zeros mean that MMX=MIQ=MJJ=0. In this case IBREM=0 at the fourth input of card 4, which indicates no bremsstrahlung photon transport calculation. KNDG=4 indicates only gamma-ray transport calculation. NGEOM=1 means plane geometry, MONOE=10 means a mono-energy problem, MNODRE=50 means a plane isotropic incidence, and IPRNT=1 means to printangular fluxes. The total energy meshes are 42, II=1 region, IQ=20 angular quadrature points. NBND=10 means to use the boundary angular flux for specifying the plane isotropic incidence. The maximum energy=10 MeV and HH=0.5 MeV energy mesh interval are specified. The spatial meshes of 70 are assigned in 41.91-cm thick plane. For KNDG=4, MAT=820 and MATERIAL=PB are inputed. The electron density is 2.7026 ($\times 10^{24}$) and the succeeding four numbers may be zeros for only a primary gamma-ray calculation. As the inputs for control the output print, all the calculated results are not stored in tape 21, 22 and 23. MRK=7 means to print both angular and scalar fluxes at seven spatial mesh points, MRKK=1 means to print $\exp(\mu x_i)I(x_i,E_j)$ at the seven mesh points, IDOS>0 means to print dose rates (mrem/h and mr/h) and absorptions (erg/g for two types of coefficients) for KNDG=4, and IEF=1 means to print fluxes in units of energy flux. The numbers of seven spatial mesh points are inputed and the last card is to specify mfp at the seven spatial mesh points for use in the calculation of buildup factors.

After the print of INPUT DATA END, integers 1,1,1 for MMX, MIQ and MJJ are printed, which is used to define the dimension of SEL. The succeeding integers 81,81,0 mean that:

LTOT=MJJ*(MMX*MIQ+40(1+MJJ)), LMAX is specified by an input

and LRES=LMAX-LTOT. For IBREM=0, the minimum LTOT requires 81, which requires the total program length of CF188 bytes. Figures 11(a) and 11(b) show the list of input data and parameters used in the calculation. Figures 12 illustrates the calculated unscattered angular energy and energy fluxes at the source energy, in which W designates the angular mesh points for Gaussian quadrature of 20 points and R the spatial mesh numbers. The R used in the energy flux spectrum designates the depth in cm in lead shield. The last output indicates the values of $\exp(\mu x)I(x,E)$ and MU*R means mfp. Figure 13 provides the scattered angular energy and energy fluxes at the source energy. Figure 14 shows dose rates and energy absorptions in units of mrem/h, mr/h, erg/g (energy transfer coefficient) and erg/g (energy absorption coefficient) represented as FDOS, as well as their respective buildup factors represented as B-F. The conversion factors used for obtaining these integrated values are given in Fig.11(b), which are automatically provided at each energy mesh by interpolating linearly the data given initially in the program.

(2) Sample problem 2: Primary gamma-ray and bremsstrahlung photon transport calculation for a plane isotropic incidence on lead

Figure 15 depicts the input data for the problem and MMX=70, MIQ=20 and MJJ=42, which requires 131040 for LTOT and the actual program length of 161810 bytes. Then 150000 is specified as the work memory for the bremsstrahlung transport calculation. Figure 16 provides the calculated energy fluxes for the bremsstrahlung photons at the first four energy meshes. Figure 17 shows the total dose rates and total energy absorptions and also respective buildup factors. Figure 18 gives the values of $\exp(\mu x)I(x,E)$ at the last 11 energy meshes, where the energy flux I(x,E) consists of those of the primary gamma ray and of the bremsstrahlung photon.

(3) Sample Problem 3: Neutron transport in air-concrete from a point isotropic ^{252}Cf source

Figure 19 provides a list of input data, in which KNDG=1 and KIN=2 because of a series calculation consisting of the energy structures of lethargy widths of 0.1, 0.2 and 0.4. NGEOM=2 means a spherical geometry, MNODRE=1 means a point isotropic source and IPRNT=1 indicates to print also angular fluxes as well as scalar fluxes. The three numbers, 27, 27 and 45 are inputed for JN(1), JN(2) and JN(3) for specifying the energy meshes in calculations with lethargy widths of, respectively, 0.1, 0.2 and 0.4. The material regions and the number of angular meshes are 6 and 20, respectively, and the fission source (Watt's formula) is specified. MSR=3 means to input the source spatial distribution only at the first three radial meshes. The source normalization is total 10^9 neutrons/sec. LTAL=10, LUT=200 and ESRN=0.005 means that the iterative calculations with maximum iteration of 200 times are required in the thermal group calculation unless the convergence criterion satisfies 0.005. The number of elements used in the scattering calculation in each material region are inputed for the six regions. The identification numbers for these regions are inputed: All the material regions except for the fourth region are the same as the first region of air, while the fourth is concrete. For specifying the output print, ITP21=ITP22=ITP23=0 and MRK=10 and IDOS=1. KR(n) for n=1,2,---,10 are inputed, and the dose rate conversion factor is inputed for the energy structures of lethargy widths of 0.1, 0.2 and 0.4.

Figures (a), (b), (c) and (d) shows the list of input print, in which two dose rate conversion factors are printed in Fig.20(d). The first data are taken from ANSI[16], contained in this program, while the other data are old ones used in Japan. Figure 21 displays only an example of output, in which the angular fluxes are printed at 10 radial meshes and also the scalar fluxes are printed at these meshes.

ACKNOWLEDGEMENT

The authors wish to express their appreciation to Mr. Y.Shindo for his help in completion of PALLAS-PL,SP-Br code.

References

1) Takeuchi K. :"Numerical Solution to Space-Angle Energy Dependent Neutron Integral Transport Equation," J. Nucl. Sci. Technol., 8, No.3, 141 (1971)

2) Takeuchi K. :"Study on a Numerical Approach to the Boltzman Transport Equation for the Purpose of Analyzing Neutron Shields," Report of Ship Res. Inst., 9, No.6 (1972) (in Japanese)

3) Sasamoto N. and Takeuchi K. :"Analysis of ^{60}Co Gamma-Ray Transport through Air by Discrete-Ordinates Transport Code," Nucl. Tech., 47 (1) 189 (1980)

4) Sasamoto N. and Takeuchi K. :"An Improvement of the PALLAS Discrete-Ordinates Transport Code," Nucl. Sci. Eng., 71, 330 (1979)

5) Takeuchi K., Tanaka S. and Kinno M. :"Transport Calculation of Gamma Rays Including Bremsstrahlung by Discrete Ordinates Code PALLAS," Nucl. Sci. Eng., 78, 273 (1981)

6) Takeuchi K.:"PALLAS-PL,SP A One Dimensional Transport Code," Papers Ship Res. Inst., No.42 (1973)

7) Bethe H. and Heitler W. :"On the Stopping of Fast Particles and on the Creation of Positive Electrons," Pro. Roy. Soc., (London), A146, 83 (1934)

8) Heitler W.:"The Quantum Theory of Radiation," p.258, 3rd ed. Oxford at the Clarendon Press (1953)

9) Tanaka S.:"EELOSS : The Program for Calculation of Electron Energy Loss Data," JAERI-M 9151 (1980)

ACKNOWLEDGEMENT

The authors wish to express their appreciation to Mr. Y.Shindo for his help in completion of PALLAS-PL,SP-Br code.

References

1) Takeuchi K. :"Numerical Solution to Space-Angle Energy Dependent Neutron Integral Transport Equation," J. Nucl. Sci. Technol., 8, No.3, 141 (1971)

2) Takeuchi K. :"Study on a Numerical Approach to the Boltzman Transport Equation for the Purpose of Analyzing Neutron Shields," Report of Ship Res. Inst., 9, No.6 (1972) (in Japanese)

3) Sasamoto N. and Takeuchi K. :"Analysis of ^{60}Co Gamma-Ray Transport through Air by Discrete-Ordinates Transport Code," Nucl. Tech., 47 (1) 189 (1980)

4) Sasamoto N. and Takeuchi K. :"An Improvement of the PALLAS Discrete-Ordinates Transport Code," Nucl. Sci. Eng., 71, 330 (1979)

5) Takeuchi K., Tanaka S. and Kinno M. :"Transport Calculation of Gamma Rays Including Bremsstrahlung by Discrete Ordinates Code PALLAS," Nucl. Sci. Eng., 78, 273 (1981)

6) Takeuchi K.:"PALLAS-PL,SP A One Dimensional Transport Code," Papers Ship Res. Inst., No.42 (1973)

7) Bethe H. and Heitler W. :"On the Stopping of Fast Particles and on the Creation of Positive Electrons," Pro. Roy. Soc., (London), A146, 83 (1934)

8) Heitler W.:"The Quantum Theory of Radiation," p.258, 3rd ed. Oxford at the Clarendon Press (1953)

9) Tanaka S.:"EELOSS : The Program for Calculation of Electron Energy Loss Data," JAERI-M 9151 (1980)

10) Koch H.W. and Motz J.W.:"Bremsstrahlung Cross-Section Formulas and Related Data," Rev. Mod. Phys., 31, No.4, 920 (1959)
11) Berger M.J. and Seltzer S.M.:"Bremsstrahlung and Photoneutrons from Thick Tungusten and Tantalum Targets," Phys. Rev., 2, No.2, 621 (1970)
12) MacFarlane R.E. et al. :"The NJOY Nuclear Data Processing System : User's Manual," LA-7584-M (1978)
13) Sasamoto N. and Takeuchi K. :"Revision of Multi-group Neutron Cross Section Libraries for PALLAS," JAERI-M 9527 (1981)
14) Nakagawa M. and Katsuragi S. : (unpublished)
and also see P.H.Kier "RIFF-RAFF, A Program for Computation of Resonance Integral in a Two Region Cell," ANL-7033 (1965)
15) Hubbell J.H. :"Photon Cross Sections, Attenuation Coefficients, and Energy Absorption Coefficients from 10 keV to 100 GeV," NSRDS-NBS 29 (1969)
16) ANSI/ANS-6.1.1 - 1977 (N666)
17) Storm E. and Harvey I.I. :"Photon Cross Sections from 0.001 to 100 MeV for Elements 1 through 100," LA-3753 (1967)
18) Theodre R. :"Reactor Shielding Design Manual," McGraw-Hill Book Company (1956)

Table 1 Subroutines used in PALLAS-PL,SP-Br

No.	Name	Function
1	BLOCKD	Initialized data.
2	PAL1D	MAIN and control the whole program.
3	DTLIST	provides the list of input data.
4	TOKYO	reads input data for a problem and prepares constants for calculation.
5	YOKHAM	reads input data for specifying nuclear data and calculates bremsstrahlung photon production cross section and pair production energy distribution.
6	READ	reads neutron cross sections from PALLAS neutron library.
7	GMXSEC	reads gamma-ray cross sections (μ_t, μ_{ph}, μ_{pp}) from PALLAS gamma-ray library.
8	EELOSS	calculates bremsstrahlung photon production cross section.
9	CONST	contains physical constants.
10	LIBRAY	contains data used for calculating the density correction factor.
11	CFDATA	contains empirical correction factors for H, C, Al, Cu, Ag as a function of electron kinetic energy.
12	CORECT	contains empirical correction factors for the elements used in PALLAS calculation, which are the interpolated values of CFDATA.
13	TWO	calculates σ_B in the kinetic energy T_k below 2 MeV.
14	THREE	calculates σ_B in the kinetic energy T_k between 2 MeV and 15 MeV.
15	RSTOP	calculates σ_B and the radiative stopping power.
16	ESTOP	calculates the ionization stopping power.
17	XNEWTN	calculates the density correction factor.

Table 1 (continued)

No.	Name	Function
18	PRINT	provides the output of data used for calculation of bremsstrahlung photon transport.
19	PAIRCR	calculates the pair production energy distribution.
20	DISTRI	calculates the pair production cross section.
21	YH	defines YH(JK, N, JDTAL) used for neutron slowing down calculation in finer energy mesh intervals if JDTAL=4.
22	ATAMI	calculates the weight function used for the numerical integration over scattering azimuthal angle ϕ.
23	HASIMA	excutes neutron thermal group calculation.
24	PSU	defines the spatial meshes in a certain material region.
25	NAGOYA	executes the neutron scattering calculation.
26	HAMATU	carrys out the neutron scattering calculation from monoenergy source.
27	HIMEJI	executes the gamma-ray scattering calculation on the basis of Klein-Nishina formula.
28	SELCT	calculates the secondary electron source.
29	PLANE	executes the transport calculation in plane geometry.
30	SPHERE	executes the transport calculation in spherical geometry.
31	OSAKA	provides the output of calculated angular and scalar fluxes as well as reaction rates.
32	SEPHOT	calculates the secondary electron source arizing from photoelectric effect.
33	BGAM	calculates the bremsstrahlung photon source.
34	SECGAM	calculates the secondary gamma-ray source produced by neutron capture reaction.

Table 2 List of identification numbers of nuclides used in PALLAS neutron and gamma-ray libraries

No.	Nuclide	Identification Number				
		Δu=0.05	Δu=0.1	Δu=0.2	Δu=0.4	Δu=0.8
1	H-1	5011	1011	2011	4011	8011
2	H-2	5012	1012	2012	4012	8012
3	Li-6	5036	1036	2036	4036	8036
4	Li-7	5037	1037	2037	4037	8037
5	Be-9	5039	1039	2039	4039	8039
6	B-10	5050	1050	2050	4050	8050
7	B-11	5051	1051	2051	4051	8051
8	C-12	5062	1062	2062	4062	8062
9	N-14	5074	1074	2074	4074	8074
10	O-16	5086	1086	2086	4086	8086
11	F	5090	1090	2090	4090	8090
12	Na-23	5113	1113	2113	4113	8113
13	Mg	5120	1120	2120	4120	8120
14	Al-27	5137	1137	2137	4137	8137
15	Si	5140	1140	2140	4140	8140
16	Ca	5200	1200	2200	4200	8200
17	Cr	5240	1240	2240	4240	8240
18	Mn-55	5255	1255	2255	4255	8255
19	Fe	5260	1260	2260	4260	8260
20	Ni	5280	1280	2280	4280	8280
21	Cu	5290	1290	2290	4290	8290
22	Zr	5400	1400	2400	4400	8400
23	Mo	5420	1420	2420	4420	8420
24	W	5740	1740	2740	4740	8740
25	Pb	5820	1820	2820	4820	8820
26	U-235	5925	1925	2925	4925	8925
27	U-238	5928	1928	2928	4928	8928
28	SUS(304)	5500	1500	2500	4500	8500
29	SUS(316)	5510	1510	2510	4510	8510
30	Ordinary Concrete	5520	1520	2520	4520	8520
31	Heavy Concrete	5530	1530	2530	4530	8530

Table 3 Energy mesh structures used in PALLAS neutron library
Lethargy-width structures of 0.05, 0.1, 0.2 and 0.4 are given.

0.05 LETHARGY WIDTH STRUCTURE

GROUP	ENERGY MESH (EV)	UPPER BOUND. (EV)	LOWER BOUND. (EV)
1	1.4200E+07	1.4559E+07	1.3849E+07
2	1.3507E+07	1.3849E+07	1.3174E+07
3	1.2849E+07	1.3174E+07	1.2531E+07
4	1.2222E+07	1.2531E+07	1.1920E+07
5	1.1626E+07	1.1920E+07	1.1339E+07
6	1.1059E+07	1.1339E+07	1.0786E+07
7	1.0520E+07	1.0786E+07	1.0260E+07
8	1.0007E+07	1.0260E+07	9.7595E+06
9	9.5185E+06	9.7595E+06	9.2835E+06
10	9.0543E+06	9.2835E+06	8.8308E+06
11	8.6127E+06	8.8308E+06	8.4001E+06
12	8.1927E+06	8.4001E+06	7.9904E+06
13	7.7931E+06	7.9904E+06	7.6007E+06
14	7.4131E+06	7.6007E+06	7.2300E+06
15	7.0515E+06	7.2300E+06	6.8774E+06
16	6.7076E+06	6.8774E+06	6.5420E+06
17	6.3805E+06	6.5420E+06	6.2229E+06
18	6.0693E+06	6.2229E+06	5.9194E+06
19	5.7733E+06	5.9194E+06	5.6307E+06
20	5.4917E+06	5.6307E+06	5.3561E+06
21	5.2239E+06	5.3561E+06	5.0949E+06
22	4.9691E+06	5.0949E+06	4.8464E+06
23	4.7268E+06	4.8464E+06	4.6101E+06
24	4.4962E+06	4.6101E+06	4.3852E+06
25	4.2770E+06	4.3852E+06	4.1714E+06
26	4.0684E+06	4.1714E+06	3.9679E+06
27	3.8700E+06	3.9679E+06	3.7744E+06
28	3.6812E+06	3.7744E+06	3.5903E+06
29	3.5017E+06	3.5903E+06	3.4152E+06
30	3.3309E+06	3.4152E+06	3.2487E+06
31	3.1684E+06	3.2487E+06	3.0902E+06
32	3.0139E+06	3.0902E+06	2.9395E+06
33	2.8669E+06	2.9395E+06	2.7961E+06
34	2.7271E+06	2.7961E+06	2.6598E+06
35	2.5941E+06	2.6598E+06	2.5301E+06
36	2.4676E+06	2.5301E+06	2.4067E+06
37	2.3472E+06	2.4067E+06	2.2893E+06
38	2.2328E+06	2.2893E+06	2.1776E+06
39	2.1239E+06	2.1776E+06	2.0714E+06
40	2.0203E+06	2.0714E+06	1.9704E+06
41	1.9218E+06	1.9704E+06	1.8743E+06
42	1.8280E+06	1.8743E+06	1.7829E+06
43	1.7389E+06	1.7829E+06	1.6959E+06
44	1.6541E+06	1.6959E+06	1.6132E+06
45	1.5734E+06	1.6132E+06	1.5346E+06
46	1.4967E+06	1.5346E+06	1.4597E+06
47	1.4237E+06	1.4597E+06	1.3885E+06
48	1.3542E+06	1.3885E+06	1.3208E+06
49	1.2882E+06	1.3208E+06	1.2564E+06
50	1.2254E+06	1.2564E+06	1.1951E+06

Table 3 (continued)

51	1.1656E+06	1.1951E+06	1.1368E+06
52	1.1088E+06	1.1368E+06	1.0814E+06
53	1.0547E+06	1.0814E+06	1.0286E+06
54	1.0032E+06	1.0286E+06	9.7848E+05
55	9.5432E+05	9.7848E+05	9.3076E+05
56	9.0778E+05	9.3076E+05	8.8536E+05
57	8.6350E+05	8.8536E+05	8.4218E+05
58	8.2139E+05	8.4218E+05	8.0111E+05
59	7.8133E+05	8.0111E+05	7.6204E+05
60	7.4322E+05	7.6204E+05	7.2487E+05
61	7.0698E+05	7.2487E+05	6.8952E+05
62	6.7250E+05	6.8952E+05	6.5589E+05
63	6.3970E+05	6.5589E+05	6.2390E+05
64	6.0850E+05	6.2390E+05	5.9348E+05
65	5.7882E+05	5.9348E+05	5.6453E+05
66	5.5059E+05	5.6453E+05	5.3700E+05
67	5.2374E+05	5.3700E+05	5.1081E+05
68	4.9820E+05	5.1081E+05	4.8590E+05
69	4.7390E+05	4.8590E+05	4.6220E+05
70	4.5079E+05	4.6220E+05	4.3966E+05
71	4.2880E+05	4.3966E+05	4.1822E+05
72	4.0789E+05	4.1822E+05	3.9782E+05
73	3.8800E+05	3.9782E+05	3.7842E+05
74	3.6907E+05	3.7842E+05	3.5996E+05
75	3.5107E+05	3.5996E+05	3.4241E+05
76	3.3395E+05	3.4241E+05	3.2571E+05
77	3.1767E+05	3.2571E+05	3.0982E+05
78	3.0217E+05	3.0982E+05	2.9471E+05
79	2.8744E+05	2.9471E+05	2.8034E+05
80	2.7342E+05	2.8034E+05	2.6667E+05
81	2.6008E+05	2.6667E+05	2.5366E+05
82	2.4740E+05	2.5366E+05	2.4129E+05
83	2.3533E+05	2.4129E+05	2.2952E+05
84	2.2385E+05	2.2952E+05	2.1833E+05
85	2.1294E+05	2.1833E+05	2.0768E+05
86	2.0255E+05	2.0768E+05	1.9755E+05
87	1.9267E+05	1.9755E+05	1.8792E+05
88	1.8328E+05	1.8792E+05	1.7875E+05
89	1.7434E+05	1.7875E+05	1.7003E+05
90	1.6584E+05	1.7003E+05	1.6174E+05
91	1.5775E+05	1.6174E+05	1.5385E+05
92	1.5005E+05	1.5385E+05	1.4635E+05
93	1.4274E+05	1.4635E+05	1.3921E+05
94	1.3577E+05	1.3921E+05	1.3242E+05
95	1.2915E+05	1.3242E+05	1.2596E+05
96	1.2285E+05	1.2596E+05	1.1982E+05
97	1.1686E+05	1.1982E+05	1.1398E+05
98	1.1116E+05	1.1398E+05	1.0842E+05
99	1.0574E+05	1.0842E+05	1.0313E+05
100	1.0058E+05	1.0313E+05	9.8101E+04

Table 3 (continued)

0.1 LETHARGY WIDTH STRUCTURE

GROUP	ENERGY MESH (EV)	UPPER BOUND. (EV)	LOWER BOUND. (EV)
1	1.4200E+07	1.4928E+07	1.3507E+07
2	1.2849E+07	1.3507E+07	1.2222E+07
3	1.1626E+07	1.2222E+07	1.1059E+07
4	1.0520E+07	1.1059E+07	1.0007E+07
5	9.5185E+06	1.0007E+07	9.0543E+06
6	8.6127E+06	9.0543E+06	8.1927E+06
7	7.7931E+06	8.1927E+06	7.4130E+06
8	7.0515E+06	7.4131E+06	6.7076E+06
9	6.3805E+06	6.7076E+06	6.0693E+06
10	5.7733E+06	6.0693E+06	5.4917E+06
11	5.2239E+06	5.4917E+06	4.9691E+06
12	4.7268E+06	4.9691E+06	4.4962E+06
13	4.2770E+06	4.4962E+06	4.0684E+06
14	3.8700E+06	4.0684E+06	3.6812E+06
15	3.5017E+06	3.6812E+06	3.3309E+06
16	3.1684E+06	3.3309E+06	3.0139E+06
17	2.8669E+06	3.0139E+06	2.7271E+06
18	2.5941E+06	2.7271E+06	2.4676E+06
19	2.3472E+06	2.4676E+06	2.2328E+06
20	2.1239E+06	2.2328E+06	2.0203E+06
21	1.9218E+06	2.0203E+06	1.8280E+06
22	1.7389E+06	1.8280E+06	1.6541E+06
23	1.5734E+06	1.6541E+06	1.4967E+06
24	1.4237E+06	1.4967E+06	1.3542E+06
25	1.2882E+06	1.3542E+06	1.2254E+06
26	1.1656E+06	1.2254E+06	1.1088E+06
27	1.0547E+06	1.1088E+06	1.0032E+06
28	9.5432E+05	1.0032E+06	9.0778E+05
29	8.6350E+05	9.0778E+05	8.2139E+05
30	7.8133E+05	8.2139E+05	7.4322E+05
31	7.0698E+05	7.4322E+05	6.7250E+05
32	6.3970E+05	6.7250E+05	6.0850E+05
33	5.7882E+05	6.0850E+05	5.5059E+05
34	5.2374E+05	5.5059E+05	4.9820E+05
35	4.7390E+05	4.9820E+05	4.5079E+05
36	4.2880E+05	4.5079E+05	4.0789E+05
37	3.8800E+05	4.0789E+05	3.6907E+05
38	3.5107E+05	3.6907E+05	3.3395E+05
39	3.1766E+05	3.3395E+05	3.0217E+05
40	2.8743E+05	3.0217E+05	2.7342E+05
41	2.6008E+05	2.7342E+05	2.4740E+05
42	2.3533E+05	2.4740E+05	2.2385E+05
43	2.1294E+05	2.2385E+05	2.0255E+05
44	1.9267E+05	2.0255E+05	1.8328E+05
45	1.7434E+05	1.8328E+05	1.6584E+05
46	1.5775E+05	1.6584E+05	1.5005E+05
47	1.4274E+05	1.5005E+05	1.3577E+05
48	1.2915E+05	1.3577E+05	1.2285E+05
49	1.1686E+05	1.2285E+05	1.1116E+05
50	1.0574E+05	1.1116E+05	1.0058E+05

Table 3 (continued)

51	9.5679E+04	1.0058E+05	9.1012E+04
52	8.6574E+04	9.1013E+04	8.2351E+04
53	7.8335E+04	8.2351E+04	7.4515E+04
54	7.0881E+04	7.4515E+04	6.7424E+04
55	6.4135E+04	6.7424E+04	6.1007E+04
56	5.8032E+04	6.1007E+04	5.5202E+04
57	5.2510E+04	5.5202E+04	4.9949E+04
58	4.7513E+04	4.9949E+04	4.5195E+04
59	4.2991E+04	4.5195E+04	4.0895E+04
60	3.8900E+04	4.0895E+04	3.7003E+04
61	3.5198E+04	3.7003E+04	3.3482E+04
62	3.1849E+04	3.3482E+04	3.0295E+04
63	2.8818E+04	3.0295E+04	2.7412E+04
64	2.6075E+04	2.7412E+04	2.4804E+04
65	2.3594E+04	2.4804E+04	2.2443E+04
66	2.1349E+04	2.2443E+04	2.0308E+04
67	1.9317E+04	2.0308E+04	1.8375E+04
68	1.7479E+04	1.8375E+04	1.6626E+04
69	1.5816E+04	1.6626E+04	1.5044E+04
70	1.4311E+04	1.5044E+04	1.3613E+04
71	1.2949E+04	1.3613E+04	1.2317E+04
72	1.1716E+04	1.2317E+04	1.1145E+04
73	1.0601E+04	1.1145E+04	1.0084E+04
74	9.5926E+03	1.0084E+04	9.1248E+03
75	8.6798E+03	9.1248E+03	8.2565E+03
76	7.8538E+03	8.2565E+03	7.4708E+03
77	7.1064E+03	7.4708E+03	6.7598E+03
78	6.4301E+03	6.7598E+03	6.1165E+03
79	5.8182E+03	6.1165E+03	5.5345E+03
80	5.2645E+03	5.5345E+03	5.0078E+03
81	4.7636E+03	5.0078E+03	4.5312E+03
82	4.3102E+03	4.5312E+03	4.1000E+03
83	3.9001E+03	4.1000E+03	3.7099E+03
84	3.5289E+03	3.7099E+03	3.3568E+03
85	3.1931E+03	3.3568E+03	3.0374E+03
86	2.8892E+03	3.0374E+03	2.7483E+03
87	2.6143E+03	2.7483E+03	2.4868E+03
88	2.3655E+03	2.4868E+03	2.2501E+03
89	2.1404E+03	2.2501E+03	2.0360E+03
90	1.9367E+03	2.0360E+03	1.8423E+03
91	1.7524E+03	1.8423E+03	1.6669E+03
92	1.5857E+03	1.6670E+03	1.5083E+03
93	1.4348E+03	1.5083E+03	1.3648E+03
94	1.2982E+03	1.3648E+03	1.2349E+03
95	1.1747E+03	1.2349E+03	1.1174E+03
96	1.0629E+03	1.1174E+03	1.0111E+03
97	9.6175E+02	1.0111E+03	9.1484E+02
98	8.7022E+02	9.1484E+02	8.2778E+02
99	7.8741E+02	8.2778E+02	7.4901E+02
100	7.1248E+02	7.4901E+02	6.7773E+02

Table 3 (continued)

0.2 LETHARGY WIDTH STRUCTURE

GROUP	ENERGY MESH (EV)	UPPER BOUND. (EV)	LOWER BOUND. (EV)
1	1.4200E+07	1.5693E+07	1.2849E+07
2	1.1626E+07	1.2849E+07	1.0520E+07
3	9.5185E+06	1.0520E+07	8.6127E+06
4	7.7931E+06	8.6127E+06	7.0515E+06
5	6.3805E+06	7.0515E+06	5.7733E+06
6	5.2239E+06	5.7733E+06	4.7268E+06
7	4.2770E+06	4.7268E+06	3.8700E+06
8	3.5017E+06	3.8700E+06	3.1684E+06
9	2.8669E+06	3.1685E+06	2.5941E+06
10	2.3472E+06	2.5941E+06	2.1239E+06
11	1.9218E+06	2.1239E+06	1.7389E+06
12	1.5734E+06	1.7389E+06	1.4237E+06
13	1.2882E+06	1.4237E+06	1.1656E+06
14	1.0547E+06	1.1656E+06	9.5432E+05
15	8.6350E+05	9.5432E+05	7.8133E+05
16	7.0698E+05	7.8133E+05	6.3970E+05
17	5.7882E+05	6.3970E+05	5.2374E+05
18	4.7390E+05	5.2374E+05	4.2880E+05
19	3.8800E+05	4.2880E+05	3.5107E+05
20	3.1767E+05	3.5107E+05	2.8744E+05
21	2.6008E+05	2.8744E+05	2.3533E+05
22	2.1294E+05	2.3533E+05	1.9267E+05
23	1.7434E+05	1.9267E+05	1.5775E+05
24	1.4274E+05	1.5775E+05	1.2915E+05
25	1.1686E+05	1.2915E+05	1.0574E+05
26	9.5679E+04	1.0574E+05	8.6574E+04
27	7.8335E+04	8.6574E+04	7.0881E+04
28	6.4135E+04	7.0881E+04	5.8032E+04
29	5.2510E+04	5.8032E+04	4.7513E+04
30	4.2991E+04	4.7513E+04	3.8900E+04
31	3.5198E+04	3.8900E+04	3.1849E+04
32	2.8818E+04	3.1849E+04	2.6076E+04
33	2.3594E+04	2.6076E+04	2.1349E+04
34	1.9317E+04	2.1349E+04	1.7479E+04
35	1.5816E+04	1.7479E+04	1.4311E+04
36	1.2949E+04	1.4311E+04	1.1717E+04
37	1.0602E+04	1.1717E+04	9.5927E+03
38	8.6798E+03	9.5927E+03	7.8538E+03
39	7.1064E+03	7.8538E+03	6.4301E+03
40	5.8182E+03	6.4302E+03	5.2646E+03
41	4.7636E+03	5.2646E+03	4.3103E+03
42	3.9001E+03	4.3103E+03	3.5289E+03
43	3.1931E+03	3.5289E+03	2.8893E+03
44	2.6143E+03	2.8893E+03	2.3655E+03
45	2.1404E+03	2.3655E+03	1.9367E+03
46	1.7524E+03	1.9367E+03	1.5857E+03
47	1.4348E+03	1.5857E+03	1.2982E+03
48	1.1747E+03	1.2982E+03	1.0629E+03
49	9.6175E+02	1.0629E+03	8.7023E+02
50	7.8741E+02	8.7023E+02	7.1248E+02

Table 3 (continued)

51	6.4468E+02	7.1248E+02	5.8333E+02
52	5.2782E+02	5.8333E+02	4.7759E+02
53	4.3214E+02	4.7759E+02	3.9102E+02
54	3.5381E+02	3.9102E+02	3.2014E+02
55	2.8967E+02	3.2014E+02	2.6211E+02
56	2.3716E+02	2.6211E+02	2.1460E+02
57	1.9417E+02	2.1460E+02	1.7570E+02
58	1.5898E+02	1.7570E+02	1.4385E+02
59	1.3016E+02	1.4385E+02	1.1777E+02
60	1.0656E+02	1.1777E+02	9.6424E+01
61	8.7248E+01	9.6424E+01	7.8945E+01
62	7.1433E+01	7.8945E+01	6.4635E+01
63	5.8484E+01	6.4635E+01	5.2919E+01
64	4.7883E+01	5.2919E+01	4.3326E+01
65	3.9203E+01	4.3326E+01	3.5472E+01
66	3.2097E+01	3.5472E+01	2.9042E+01
67	2.6279E+01	2.9042E+01	2.3778E+01
68	2.1515E+01	2.3778E+01	1.9468E+01
69	1.7615E+01	1.9468E+01	1.5939E+01
70	1.4422E+01	1.5939E+01	1.3050E+01
71	1.1808E+01	1.3050E+01	1.0684E+01
72	9.6673E+00	1.0684E+01	8.7474E+00
73	7.9150E+00	8.7474E+00	7.1617E+00
74	6.4802E+00	7.1617E+00	5.8635E+00
75	5.3056E+00	5.8635E+00	4.8007E+00
76	4.3438E+00	4.8007E+00	3.9304E+00
77	3.5564E+00	3.9304E+00	3.2180E+00
78	2.9117E+00	3.2180E+00	2.6347E+00
79	2.3839E+00	2.6347E+00	2.1571E+00
80	1.9518E+00	2.1571E+00	1.7661E+00
81	1.5980E+00	1.7661E+00	1.4459E+00
82	1.3083E+00	1.4459E+00	1.1838E+00
83	1.0712E+00	1.1838E+00	9.6924E-01
84	8.7701E-01	9.6924E-01	7.9355E-01
85	7.1804E-01	7.9355E-01	6.4971E-01
86	5.8788E-01	6.4971E-01	5.3194E-01
87	4.8131E-01	5.3193E-01	4.3551E-01
88	3.9406E-01	4.3551E-01	0.0

Table 3 (continued)

0.4 LETHARGY WIDTH STRUCTURE

GROUP	ENERGY MESH (EV)	UPPER BOUND. (EV)	LOWER BOUND. (EV)
1	1.4200E+07	1.7344E+07	1.1626E+07
2	9.5185E+06	1.1626E+07	7.7931E+06
3	6.3805E+06	7.7931E+06	5.2239E+06
4	4.2770E+06	5.2239E+06	3.5017E+06
5	2.8669E+06	3.5017E+06	2.3472E+06
6	1.9218E+06	2.3472E+06	1.5734E+06
7	1.2882E+06	1.5734E+06	1.0547E+06
8	8.6350E+05	1.0547E+06	7.0698E+05
9	5.7882E+05	7.0698E+05	4.7390E+05
10	3.8800E+05	4.7390E+05	3.1767E+05
11	2.6008E+05	3.1767E+05	2.1294E+05
12	1.7434E+05	2.1294E+05	1.4274E+05
13	1.1686E+05	1.4274E+05	9.5679E+04
14	7.8335E+04	9.5679E+04	6.4136E+04
15	5.2510E+04	6.4135E+04	4.2991E+04
16	3.5198E+04	4.2991E+04	2.8818E+04
17	2.3594E+04	2.8818E+04	1.9317E+04
18	1.5816E+04	1.9317E+04	1.2949E+04
19	1.0602E+04	1.2949E+04	8.6798E+03
20	7.1064E+03	8.6798E+03	5.8182E+03
21	4.7636E+03	5.8182E+03	3.9001E+03
22	3.1931E+03	3.9001E+03	2.6143E+03
23	2.1404E+03	2.6143E+03	1.7524E+03
24	1.4348E+03	1.7524E+03	1.1747E+03
25	9.6175E+02	1.1747E+03	7.8741E+02
26	6.4468E+02	7.8741E+02	5.2782E+02
27	4.3214E+02	5.2782E+02	3.5381E+02
28	2.8967E+02	3.5381E+02	2.3716E+02
29	1.9417E+02	2.3716E+02	1.5898E+02
30	1.3016E+02	1.5898E+02	1.0656E+02
31	8.7248E+01	1.0656E+02	7.1433E+01
32	5.8484E+01	7.1433E+01	4.7883E+01
33	3.9203E+01	4.7883E+01	3.2097E+01
34	2.6279E+01	3.2097E+01	2.1515E+01
35	1.7615E+01	2.1515E+01	1.4422E+01
36	1.1808E+01	1.4422E+01	9.6673E+00
37	7.9150E+00	9.6673E+00	6.4802E+00
38	5.3056E+00	6.4802E+00	4.3438E+00
39	3.5564E+00	4.3438E+00	2.9117E+00
40	2.3839E+00	2.9117E+00	1.9518E+00
41	1.5980E+00	1.9518E+00	1.3083E+00
42	1.0712E+00	1.3083E+00	8.7701E-01
43	7.1804E-01	8.7701E-01	5.8788E-01
44	4.8131E-01	5.8787E-01	3.9406E-01
45	3.2263E-01	3.9407E-01	0.0

Table 4 Secondary gamma-ray energy structure

No.	E(MeV)	No.	E(MeV)	No.	E(MeV)
1	13.0	11	1.0	21	0.075
2	10.0	12	0.5	22	0.068
3	8.0	13	0.34	23	0.062
4	7.0	14	0.24	24	0.058
5	6.0	15	0.18	25	0.052
6	5.0	16	0.15		
7	4.0	17	0.125		
8	3.0	18	0.108		
9	2.0	19	0.094		
10	1.5	20	0.083		

Table 6 Legendre expansion orders and lower bounds of neutron energy

Nuclide	Order	E(MeV)	Nuclide	Order	E(MeV)
H-1	-	-	Si	10	0.106
H-2	6	0.106	Ca	10	0.106
Li-6	8	0.106	Cr	15	0.106
Li-7	9	0.213	Mn-55	15	0.640
Be-9	8	0.158	Fe	11	0.318
B-10	8	0.158	Ni	12	0.106
B-11	8	0.158	Cu	12	0.106
C-12	6	0.106	Zr	15	0.106
N-14	10	1.17	Mo	14	0.106
O-16	10	0.106	W	19	0.106
F	10	0.106	Pb	14	0.260
Na-23	14	0.106	U-235	15	0.215
Mg	15	0.106	U-238	15	0.106
Al-27	10	0.213			

Table 5 Angular quadrature sets fixed in the code

	16		20		28	
n	ω_n	$\Delta\omega_n$	ω_n	$\Delta\omega_n$	ω_n	$\Delta\omega_n$
1	0.9894	0.02715	0.9931	0.01761	0.9950	0.010
2	0.9446	0.06225	0.9640	0.04060	0.9835	0.013
3	0.8656	0.09516	0.9122	0.06267	0.9685	0.017
4	0.7554	0.12463	0.8391	0.08328	0.9495	0.021
5	0.6179	0.14960	0.7463	0.10193	0.9260	0.026
6	0.4580	0.16916	0.6361	0.11819	0.8970	0.032
7	0.2816	0.18260	0.5109	0.13169	0.8620	0.038
8	0.0950	0.18945	0.3737	0.14096	0.8210	0.044
9			0.2278	0.14917	0.7740	0.050
10			0.0765	0.15275	0.7210	0.056
11					0.6610	0.064
12	Symmetry				0.5930	0.072
13					0.5170	0.080
14					0.4335	0.087
15			Symmetry		0.3450	0.090
16					0.2525	0.095
17					0.1550	0.100
18					0.0525	0.105
19					-0.0525	0.105
20					-0.1575	0.105
21					-0.2625	0.105
22					-0.3675	0.105
23					-0.4725	0.105
24					-0.5750	0.100
25					-0.6750	0.100
26					-0.7725	0.095
27					-0.8675	0.095
28					-0.9575	0.085

Table 7 PALLAS-PL,SP-Br file requirement

Logical unit	Contents	Remarks
1	Neutron library	Neutron cross sections are read from PALLAS library.
2	Gamma-ray library	Gamma-ray cross sections are read from PALLAS library.
3	Work for SEL	
5	Input	
6	Output	
8	Work for WG	WG(30,30,10) for non-hydrogen
9	Work for CIB	
10	Work for FN	Angular flux (150,30)
11	Work for FN	Scattered angular flux at source energy for MONOE>0 gamma ray.
12	Work for CIA	Inelastic scattering matrix
13	Work for WT	WT(30,30,30) for hydrogen
14	Work for FN	Angular flux for MONOE>0 neutron
15	Work for KDATA	Various data for electron cross sections
19	Work for SG	Secondary photon source
21	Angular flux	Angular flux is stored if ITP21>0.
22	Scalar flux	Scalar flux is stored if ITP22>0.
23	Reaction	Reaction is stored if ITP23>0.

Table 8 Relation of main variables to program mnemonics

COMMON(DIMENSION)	COMMENT
/AAA/	
WP(30)	ω_p; angular quadrature points
WWP(30)	$\Delta\omega_p$; angular quadrature weights
WBP(29)	Boundaries of ω_p ranges
/AA1/	
BP1(20)	Gaussian quadrature of 20 points
BW1(20)	Weights for BP1(20)
BB1(19)	Boundaries of BP1(20)
BP2(20)	Gaussian quadrature of 16 points
BW2(20)	Weights for BP2
BB2(19)	Boundaries of BP2
BP3(30)	Tailored quadrature of 28 mesh points for detailed angular flux calculation for a point source
BW3(30)	Weights for BP3
BB3(30)	Boundaries of BP3
/CCC/	
AMU(10,20)	μ_m; angular quadrature of neutron elastic scattering angle
WAMU(10,20)	Weights for μ_m
/AMU/	
AMAS(30)	A_i; Mass number of i-th nuclide
SIGT(120)	$\sigma_t(E_j)$; microscopic total cross section

Table 8 (continued)

COMMON(DIMENSION)	COMMENT
FMU(80,20)	$f_\ell(E_j)$; ℓ-order of Legendre coefficient
CIB(80,80)	Inelastic scattering slowing down cross section
/DDD/	
JJ	Total number of energy meshes
HH	Lethargy width or energy mesh interval
IQ	Number of angular meshes
II	Number of material regions
EMAX	Maximum energy in MeV
E(120)	Energy in MeV at energy meshes
/EEE/	
MES(20)	Number of meshes in each material region
DR(20)	Spatial mesh interval in each region
NGEOM	Geometry
/FFF/	
FN(150,30)	Angular flux (Spatial meshes, angular meshes)
SN(150,30)	Angular source
CRT(20,120)	Macroscopic total cross section
RD(600)	Radial distances in cm (r_i)
MS	
/GGG/	
NOEL(20)	Number of elements in each material region
NEK(20)	Identification numbers in material regions

Table 8 (continued)

COMMOM(DIMENSION)	COMMENT
ALPH(10,20)	α_{ij}; cosine of i-th scattering angle for j-th nuclide
ALHY(120)	α_i; the same as above for hydrogen
/GAMA/	
WAVE(120)	λ_j; wavelength of photon
DWAVE(119)	$\Delta\lambda_j$; width of j-th wavelength
SG(150,30)	Secondary photon source
GMU	$\mu = 1+\lambda_k-\lambda_j$; cosine of scattering angle
JPP	for pair production
/HHH/	
FGM(10,80,20)	$\Sigma_{el}(E_j)f_\ell(E_j)$ for non-hydrogeneous nuclide
KMAX(20)	Maximum number of energy meshes concrening to max. slowing down in elastic scattering
KK(30,20)	Number of ℓ belonging to k-th slowing down
SIGMA(120,30)	macroscopic elastic scattering cross section
/III/	
MDT	Number of angular meshes in elastic scattering
WT(30,30,30)	w_n; weight for ψ_n
/JJJ/	
RO(30)	$1/A_i$; A_i is mass number.
SR(300)	Source spatial distribution
SE(120)	Source energy distribution
/LLL/	

Table 8 (continued)

COMMON (DIMENSION)	COMMENT
A(20)	$2\pi\Delta\mu_1\Sigma_{el}(E_j)f_1(E_j)$
MA	
MYR	
MRR	Total number of spatial meshes
IPQK	Number of angular meshes for $\omega>0$.

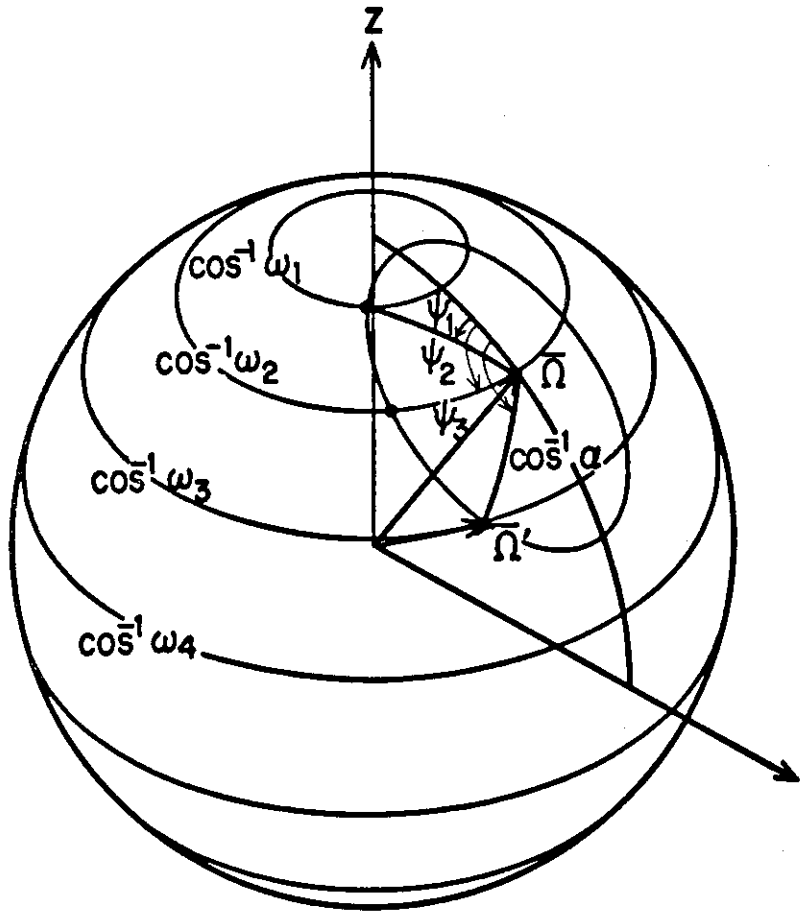

Fig. 1 Relation between azimuthal angle of scattering ψ and directional cosine ω_n in scattering

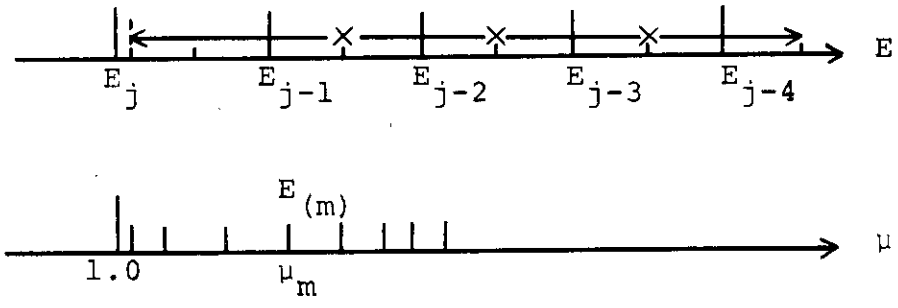

Fig.2 Energy mesh assignment and relation between energy points $E(\mu_m)$ and energy region of each energy mesh

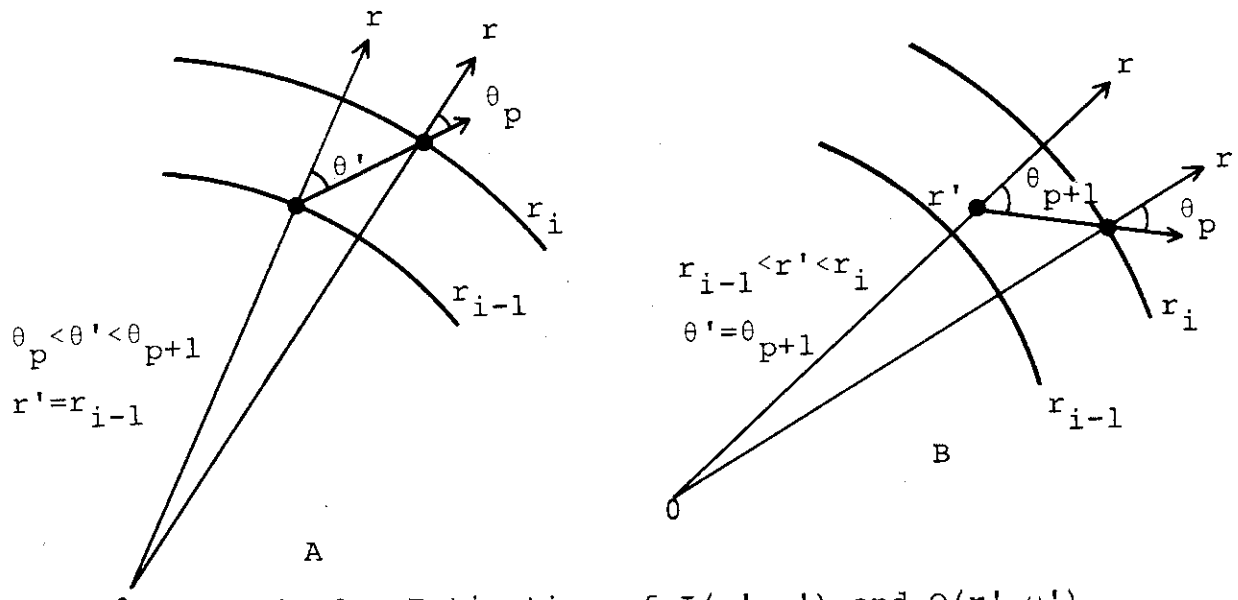

Fig.3 Estimation of $I(r',\omega')$ and $Q(r',\omega')$ in spherical geometry

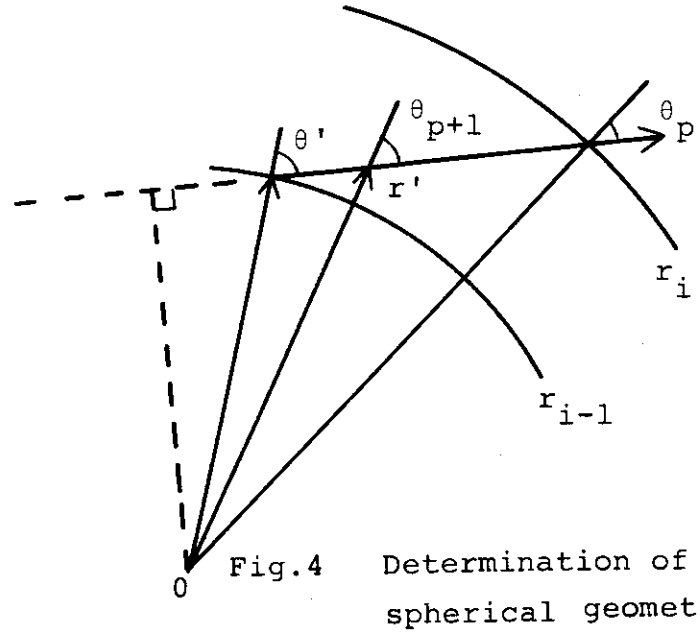

Fig.4 Determination of (r',θ') in spherical geometry

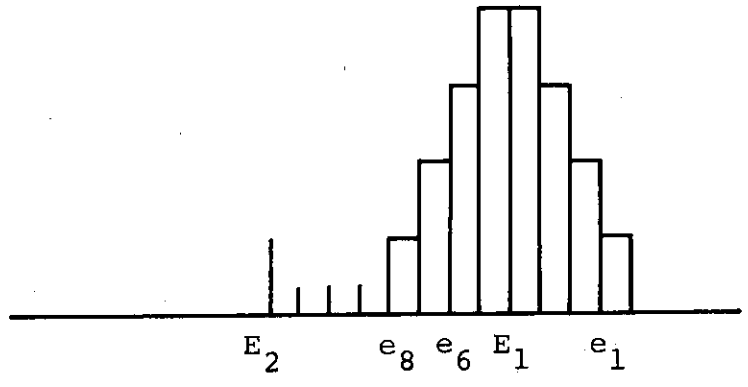

Fig.5 Neutron mono-energy source calculation scheme

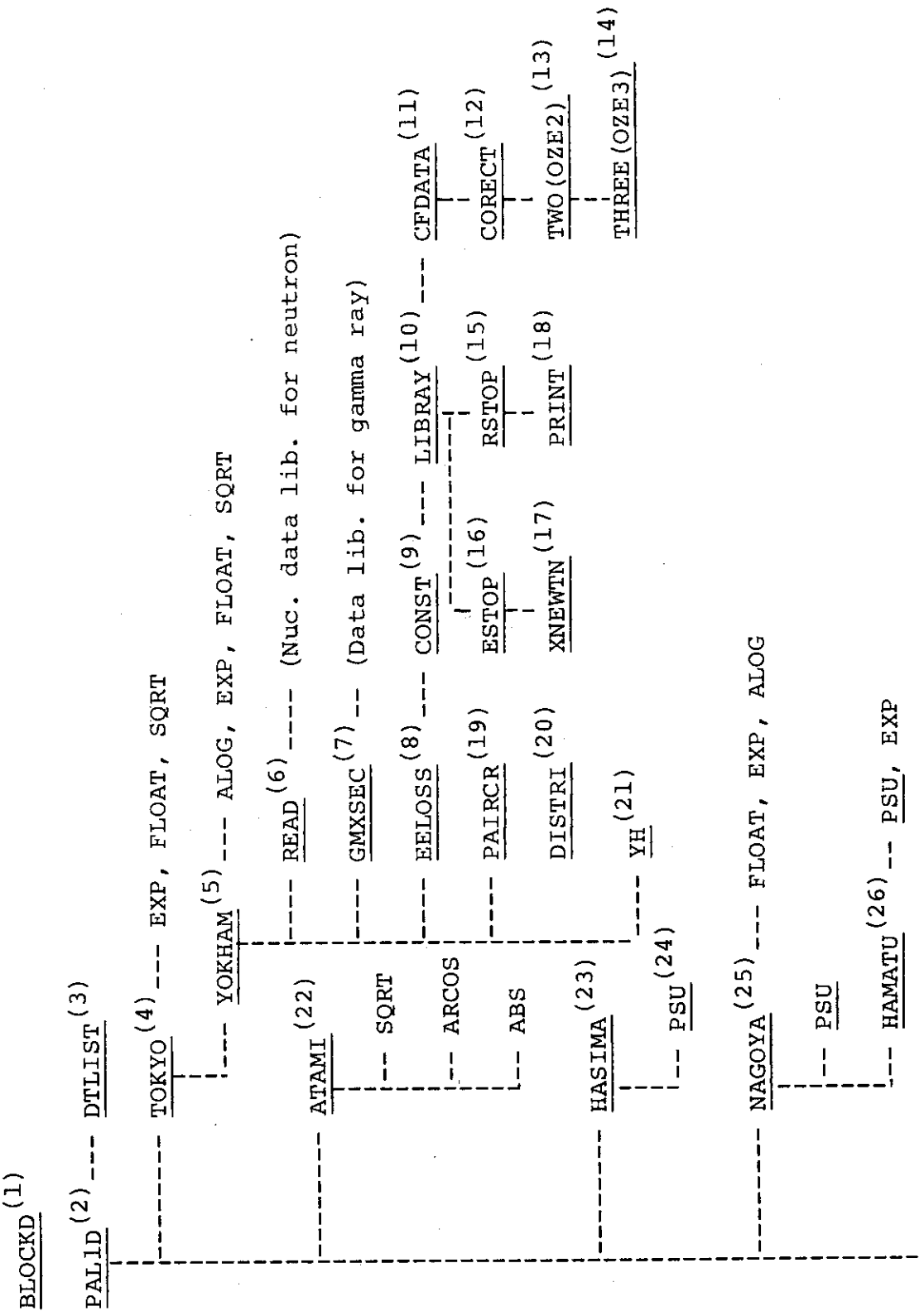

Fig.6-1 Structure map No.1

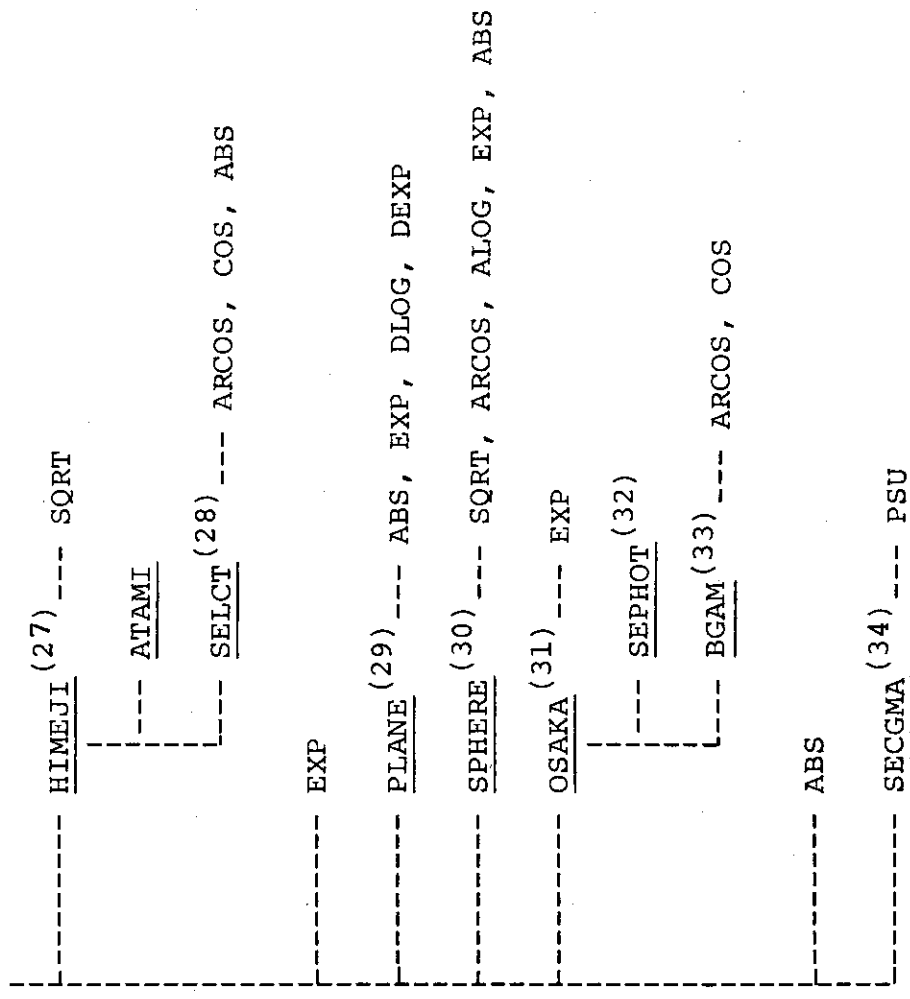

Fig.6-2 Structure map No.2

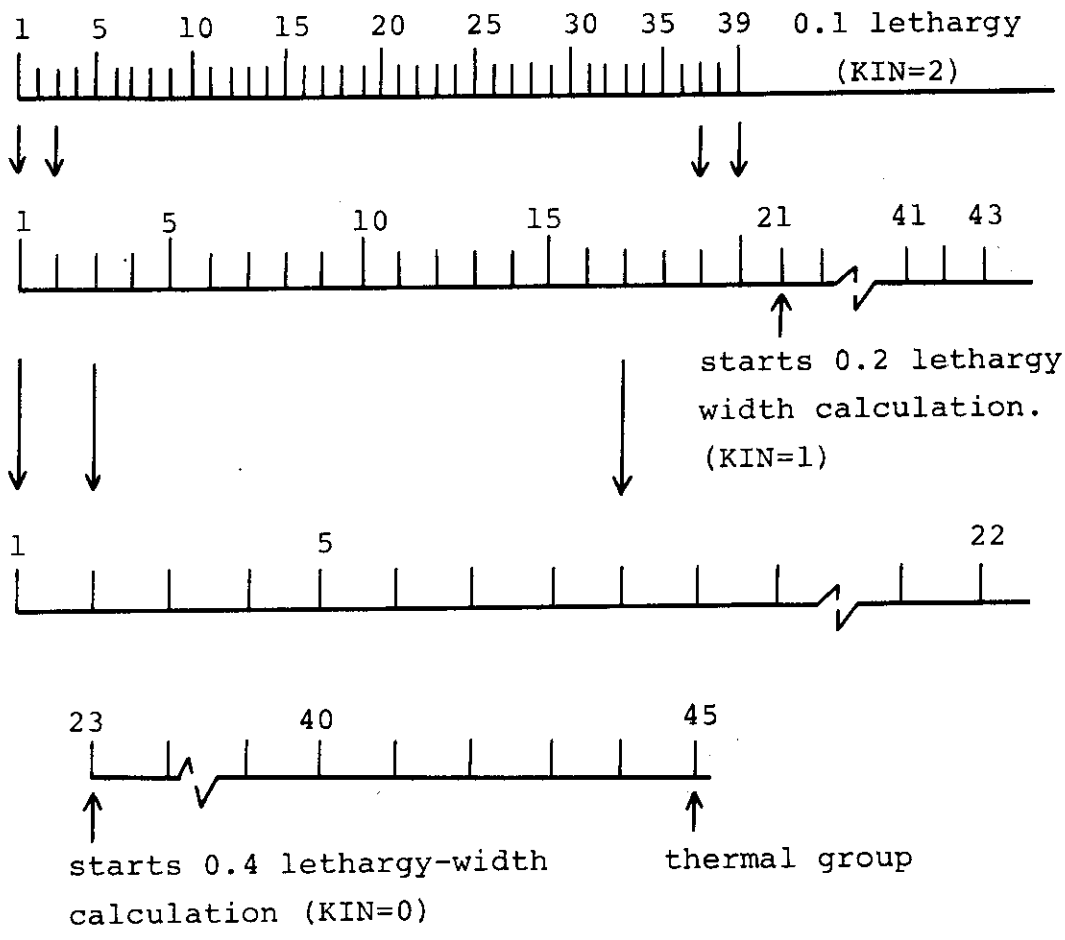

Fig.7 An example of a series calculation by a combination of energy structures of 0.1, 0.2 and 0.4 lethargy widths.

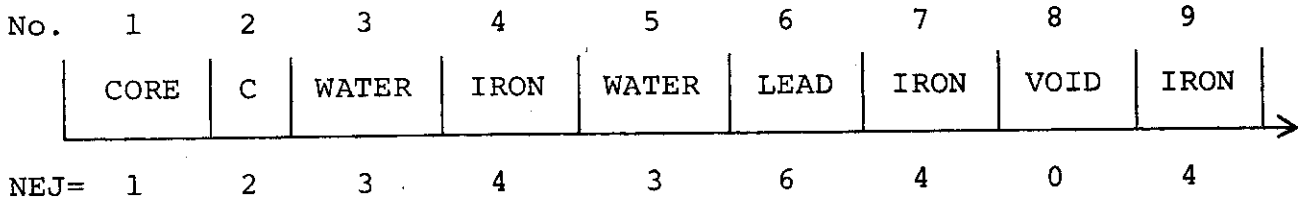

Fig.8 An example of assignment of identification numbers of material regions

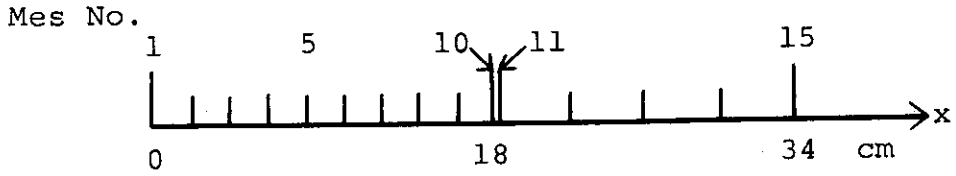

i	1	2
MES(i)	10	5
RR(i)	18.0	16.0

(A) Plane geometry

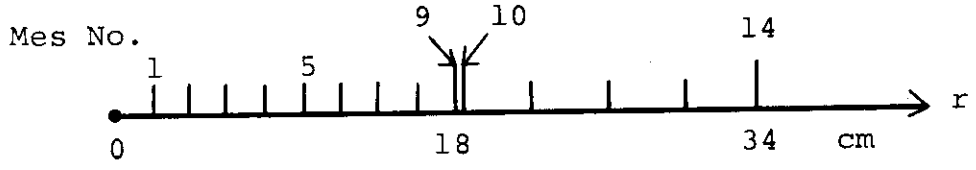

i	1	2
MES(i)	9	5
RR(i)	18.0	16.0

(B-1) Spherical geometry (NBND=0)

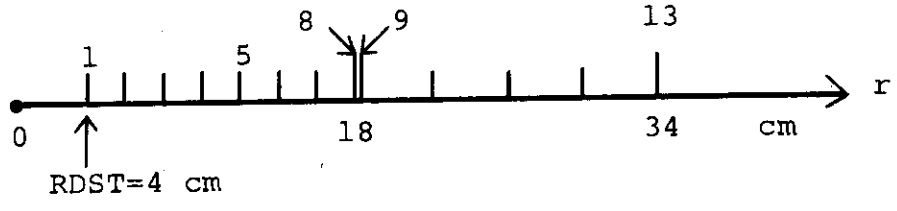

i	1	2
MES(i)	8	5
RR(i)	14.0	16.0

(B-2) Spherical geometry (NBND=10)

Fig.9 Spatial mesh assinment

```
                    **********************
                    *                    *
                    *  INPUT DATA LIST   *
                    *                    *
                    **********************

        ....*....1....*....2....*....3....*....4....*....5....*....6....*....7....*....8
 1        0  0  0                                                                        1
 2       LEAD(10 MEV)  PLANE ISOTROPIC  81-7-31,TEST OF HH PARAMETER OPTION             2
 3        4  0  0  0                                                                     3
 4        1 10 50  0  1                                                                 4
 5       42                                                                             5
 6        1 20  0                                                                       6
 7       10                                                                             7
 8       10.0        0.5                                                                8
 9       70                                                                             9
10       41.91                                                                         10
11      820PB                                                                          11
12       2.7026     82.0       0.0330     11.34      0.088                            12
13        0  0  0                                                                     13
14        7  1  4  1  0                                                               14
15        4  7 13 22 31 46 61                                                         15
16       1.00       2.00       4.00       7.00       10.0       15.0       20.0      16
        ....*....1....*....2....*....3....*....4....*....5....*....6....*....7....*....8

        *** INPUT DATA END ***

MMX,MIQ,MJJ =     1     1     1

LTOT,LMAX,LRES =          81          81           0
```

Fig. 10 List of input data for sample problem 1

```
                    INPUT  DATA
*** LEAD(10 MEV)  PLANE ISOTROPIC  81-7-31,TEST OF HH PARAMETER OPTION            ***

KNDG,KIN,NORF,KTST  =    4    0    0    0

NGEOM,MONOE,MNODRE,IBREM,IPRNT =    1   10   50    0    1

          ONE DIMENSIONAL PLANE GEOMETRY

  ENERGY MESH =  42    MATERIAL REGION =  1    ANGULAR MESH = 20    FISSION = 0    JSTAT= 0

   NBND = 10    MSR =  0    IQ1Q = 0    JDTAL = 0

   E-MAX = 1.000E+01 MEV    LETHARGY WIDTH = 5.000E-01  SOURCE NORM. = 1.000E+00  RDST = 0.0
   E(MEV) = 1.000E+01 9.500E+00 9.000E+00 8.500E+00 8.000E+00 7.500E+00 7.000E+00 6.500E+00 6.000E+00 5.500E+00
   E(MEV) = 5.000E+00 4.500E+00 4.000E+00 3.500E+00 3.000E+00 2.500E+00 2.000E+00 1.500E+00 1.160E+00 9.451E-01
   E(MEV) = 7.619E-01 6.086E-01 4.824E-01 3.799E-01 2.977E-01 2.324E-01 1.893E-01 1.597E-01 1.381E-01 1.217E-01
   E(MEV) = 1.087E-01 9.829E-02 8.967E-02 8.243E-02 7.628E-02 7.098E-02 6.637E-02 6.233E-02 5.874E-02 5.466E-02
   E(MEV) = 5.085E-02 4.754E-02
   WAVE(J) = 5.110E-02 5.379E-02 5.678E-02 6.012E-02 6.387E-02 6.813E-02 7.300E-02 7.862E-02 8.517E-02 9.291E-02
   WAVE(J) = 1.022E-01 1.136E-01 1.277E-01 1.460E-01 1.703E-01 2.044E-01 2.555E-01 3.407E-01 4.407E-01 5.407E-01
   WAVE(J) = 6.707E-01 8.397E-01 1.059E+00 1.345E+00 1.716E+00 2.199E+00 2.699E+00 3.199E+00 3.699E+00 4.199E+00
   WAVE(J) = 4.699E+00 5.199E+00 5.699E+00 6.199E+00 6.699E+00 7.199E+00 7.699E+00 8.199E+00 8.699E+00 9.349E+00
   WAVE(J) = 1.005E+01 1.075E+01
   DWAVE(J) = 2.689E-03 2.988E-03 3.340E-03 3.757E-03 4.258E-03 4.867E-03 5.615E-03 6.551E-03 7.742E-03 9.291E-03
   DWAVE(J) = 1.136E-02 1.419E-02 1.825E-02 2.433E-02 3.407E-02 5.110E-02 8.517E-02 1.000E-01 1.000E-01 1.300E-01
   DWAVE(J) = 1.690E-01 2.197E-01 2.856E-01 3.713E-01 4.827E-01 5.000E-01 5.000E-01 5.000E-01 5.000E-01 5.000E-01
   DWAVE(J) = 5.000E-01 5.000E-01 5.000E-01 5.000E-01 5.000E-01 5.000E-01 5.000E-01 5.000E-01 6.500E-01 7.000E-01
   DWAVE(J) = 7.000E-01

REGION              1         2         3         4         5         6         7         8         9        10
   MESHES =        70
   THICKNESS =  4.191E+01

ANGULAR QUADATURE CONSTANTS COSINE AND WEIGHT
 W-P=   0.99312   0.96397   0.91223   0.83911   0.74633   0.63605   0.51086   0.37370   0.22778   0.07652
 W-P=  -0.07652  -0.22778  -0.37370  -0.51086  -0.63605  -0.74663  -0.83911  -0.91223  -0.96397  -0.99312
WW-P=   0.01761   0.04060   0.06267   0.08328   0.10193   0.11819   0.13169   0.14210   0.14917   0.15275
WW-P=   0.15275   0.14917   0.14210   0.13169   0.11819   0.10193   0.08328   0.06267   0.04060   0.01761

NO OF ELEMENTS IN EACH REGION=  1

IDENTIFICATION OF REGION=  1

INNER BOUNDARY CONDITION BOUND(W-Q,E-J)
 0.160E+00 0.165E+00 0.174E+00 0.190E+00 0.213E+00 0.250E+00 0.312E+00 0.426E+00 0.699E+00 0.208E+01
RMES(CM)= 0.0       6.074E-01 1.215E+00 1.822E+00 2.430E+00 3.037E+00 3.644E+00 4.252E+00 4.859E+00 5.467E+00
RMES(CM)= 6.074E+00 6.681E+00 7.289E+00 7.896E+00 8.503E+00 9.111E+00 9.718E+00 1.033E+01 1.093E+01 1.154E+01
RMES(CM)= 1.215E+01 1.276E+01 1.336E+01 1.397E+01 1.458E+01 1.518E+01 1.579E+01 1.640E+01 1.701E+01 1.761E+01
RMES(CM)= 1.822E+01 1.883E+01 1.944E+01 2.004E+01 2.065E+01 2.126E+01 2.187E+01 2.247E+01 2.308E+01 2.369E+01
RMES(CM)= 2.430E+01 2.490E+01 2.551E+01 2.612E+01 2.673E+01 2.733E+01 2.794E+01 2.855E+01 2.915E+01 2.976E+01
RMES(CM)= 3.037E+01 3.098E+01 3.158E+01 3.219E+01 3.280E+01 3.341E+01 3.401E+01 3.462E+01 3.523E+01 3.584E+01
RMES(CM)= 3.644E+01 3.705E+01 3.766E+01 3.827E+01 3.887E+01 3.948E+01 4.009E+01 4.070E+01 4.130E+01 4.191E+01

RADIUS(CM)=
RD= 0.0       6.074E-01 1.215E+00 1.822E+00 2.430E+00 3.037E+00 3.644E+00 4.252E+00 4.859E+00 5.467E+00
RD= 6.074E+00 6.681E+00 7.289E+00 7.896E+00 8.503E+00 9.111E+00 9.718E+00 1.033E+01 1.093E+01 1.154E+01
RD= 1.215E+01 1.276E+01 1.336E+01 1.397E+01 1.458E+01 1.518E+01 1.579E+01 1.640E+01 1.701E+01 1.761E+01
RD= 1.822E+01 1.883E+01 1.944E+01 2.004E+01 2.065E+01 2.126E+01 2.187E+01 2.247E+01 2.308E+01 2.369E+01
RD= 2.430E+01 2.490E+01 2.551E+01 2.612E+01 2.673E+01 2.733E+01 2.794E+01 2.855E+01 2.915E+01 2.976E+01
```

Fig. 11(a) List of input and constants for calculation for sample problem 1

```
RD= 3.037E+01 3.098E+01 3.158E+01 3.219E+01 3.280E+01 3.341E+01 3.401E+01 3.462E+01 3.523E+01 3.584E+01
RD= 3.644E+01 3.705E+01 3.766E+01 3.827E+01 3.887E+01 3.948E+01 4.009E+01 4.070E+01 4.130E+01 4.191E+01

DR(CM)= 6.074E-01


 ***** NUCLEAR DATA   *****

 REGION NO = 1    MATERIAL =PB

 ELECTRON DENSITY =    2.7026  ZN(I) = 8.200E+01  ATOMIC DENSITY= 3.300E-02
MATERIAL DENSITY = 1.134E+01  K-SHELL BINDING ENERGY= 8.800E-02 (MEV)

 JPHOT,JPPA,MAT(I)  =   0    0  820

REGION = 1
SIGMATT= 0.5489     0.5422     0.5353     0.5281     0.5205     0.5140     0.5072     0.4999     0.4922     0.4867
SIGMATT= 0.4808     0.4754     0.4695     0.4705     0.4717     0.4887     0.5103     0.5783     0.7007     0.8263
SIGMATT=  1.028      1.338      1.850      2.755      4.417      7.671      12.23      18.42      26.35      36.23
SIGMATT=  48.05      55.21      37.70      26.58      26.62      32.21      38.47      45.43      53.17      64.49
SIGMATT=  78.25      93.68
SIGMAPP= 0.4055     0.3919     0.3780     0.3638     0.3494     0.3352     0.3167     0.3000     0.2828     0.2624
SIGMAPP= 0.2417     0.2160     0.1905     0.1595     0.1298     0.8899E-01 0.5604E-01 0.1865E-01 0.3344E-05 0.0
SIGMAPP= 0.0        0.0        0.0        0.0        0.0        0.0        0.0        0.0        0.0        0.0
SIGMAPP= 0.0        0.0        0.0        0.0        0.0        0.0        0.0        0.0        0.0        0.0
SIGMAPP= 0.0        0.0

MRK,MRKK,IDOS,IEF,ICUR =    7    1    4    1    0

ENERGY FLUX TO MREM/HR CONVERSION FACTOR
DOSE(J,N) =    9.550E-04  9.674E-04  9.806E-04  9.948E-04  1.010E-03  1.030E-03  1.051E-03  1.074E-03  1.100E-03  1.128E-03
DOSE(J,N) =    1.160E-03  1.211E-03  1.270E-03  1.329E-03  1.400E-03  1.495E-03  1.620E-03  1.750E-03  1.893E-03  2.010E-03
DOSE(J,N) =    2.128E-03  2.261E-03  2.359E-03  2.472E-03  2.530E-03  2.517E-03  2.514E-03  2.526E-03  2.588E-03  2.681E-03
DOSE(J,N) =    2.765E-03  2.860E-03  3.028E-03  3.190E-03  3.420E-03  3.693E-03  3.968E-03  4.244E-03  4.562E-03  5.079E-03
DOSE(J,N) =    5.656E-03  6.427E-03

ENERGY FLUX TO MR/HR CONVERSION FACTOR
DOSE(J,N) =    1.000E-03  1.009E-03  1.019E-03  1.029E-03  1.040E-03  1.055E-03  1.072E-03  1.090E-03  1.110E-03  1.143E-03
DOSE(J,N) =    1.180E-03  1.213E-03  1.250E-03  1.304E-03  1.370E-03  1.457E-03  1.570E-03  1.710E-03  1.804E-03  1.875E-03
DOSE(J,N) =    1.927E-03  1.958E-03  1.968E-03  1.951E-03  1.907E-03  1.827E-03  1.756E-03  1.686E-03  1.637E-03  1.602E-03
DOSE(J,N) =    1.572E-03  1.555E-03  1.579E-03  1.602E-03  1.672E-03  1.769E-03  1.865E-03  1.960E-03  2.088E-03  2.339E-03
DOSE(J,N) =    2.620E-03  3.013E-03

ENERGY TRANSFER COEFF. -- ERG/G CONV.FACTOR
DOSE(J,N) =    6.712E-08  6.555E-08  6.394E-08  6.227E-08  6.056E-08  5.878E-08  5.694E-08  5.502E-08  5.303E-08  5.108E-08
DOSE(J,N) =    4.902E-08  4.709E-08  4.502E-08  4.342E-08  4.165E-08  4.158E-08  4.149E-08  4.614E-08  5.647E-08  6.739E-08
DOSE(J,N) =    8.597E-08  1.159E-07  1.682E-07  2.617E-07  4.315E-07  7.376E-07  1.144E-06  1.630E-06  2.132E-06  2.633E-06
DOSE(J,N) =    3.176E-06  3.597E-06  3.315E-06  3.077E-06  3.413E-06  4.156E-06  4.995E-06  5.933E-06  6.953E-06  8.369E-06
DOSE(J,N) =    1.008E-05  1.202E-05

ENERGY ABSORPTION COEFF. -- ERG/G CONV.FACTOR
DOSE(J,N) =    4.966E-08  4.906E-08  4.843E-08  4.778E-08  4.710E-08  4.628E-08  4.543E-08  4.453E-08  4.357E-08  4.257E-08
DOSE(J,N) =    4.149E-08  4.042E-08  3.925E-08  3.842E-08  3.749E-08  3.792E-08  3.845E-08  4.341E-08  5.354E-08  6.423E-08
DOSE(J,N) =    8.231E-08  1.116E-07  1.627E-07  2.548E-07  4.218E-07  7.256E-07  1.130E-06  1.615E-06  2.117E-06  2.622E-06
DOSE(J,N) =    3.170E-06  3.595E-06  3.307E-06  3.062E-06  3.393E-06  4.130E-06  4.962E-06  5.892E-06  6.904E-06  8.320E-06
DOSE(J,N) =    1.003E-05  1.197E-05
```

Fig. 11(b) List of input and constants for calculation for sample problem 1

OUTPUT OF THE COMPUTATION

** UNSCATTERED FLUX ***

RADIATION ENERGY = 0.1000E+02MEV

ANGULAR FLUXES OF RADIATION N/CM**2.SEC.MEV.SR OR IEF=1 E.N/CM**2.SEC.MEV.SR IEF= 1

W/R	4	7	13	22	31	46	61
0.99312	5.8542E-01	2.1385E-01	2.8537E-02	1.3911E-03	6.7811E-05	4.4110E-07	2.8693E-09
0.96397	5.8503E-01	2.0730E-01	2.6028E-02	1.1580E-03	5.1521E-05	2.8780E-07	1.6077E-09
0.91223	5.8288E-01	1.9474E-01	2.1736E-02	8.1056E-04	3.0226E-05	1.2581E-07	5.2367E-10
0.83911	5.7594E-01	1.7489E-01	1.6125E-02	4.5148E-04	1.2641E-05	3.2633E-08	8.4243E-11
0.74633	5.5836E-01	1.4620E-01	1.0023E-02	1.7992E-04	3.2298E-06	3.9748E-09	4.8917E-12
0.63605	5.1934E-01	1.0779E-01	4.6433E-03	4.1515E-05	3.7117E-07	1.4295E-10	5.5058E-14
0.51086	4.3984E-01	6.2098E-02	1.2378E-03	3.4833E-06	9.8024E-09	5.4984E-13	3.0842E-17
0.37370	2.9310E-01	2.0172E-02	9.5541E-05	3.1143E-08	1.0152E-11	1.5673E-17	2.4197E-23
0.22778	8.6587E-02	1.0730E-03	1.6478E-07	3.1358E-13	5.9675E-19	1.7440E-28	5.0966E-38
0.07652	4.3838E-05	9.2395E-11	4.1045E-22	3.8430E-39	3.5981E-56	0.0	0.0
-0.07652	0.0	0.0	0.0	0.0	0.0	0.0	0.0
-0.22778	0.0	0.0	0.0	0.0	0.0	0.0	0.0
-0.37370	0.0	0.0	0.0	0.0	0.0	0.0	0.0
-0.51086	0.0	0.0	0.0	0.0	0.0	0.0	0.0
-0.63605	0.0	0.0	0.0	0.0	0.0	0.0	0.0
-0.74663	0.0	0.0	0.0	0.0	0.0	0.0	0.0
-0.83911	0.0	0.0	0.0	0.0	0.0	0.0	0.0
-0.91223	0.0	0.0	0.0	0.0	0.0	0.0	0.0
-0.96397	0.0	0.0	0.0	0.0	0.0	0.0	0.0
-0.99312	0.0	0.0	0.0	0.0	0.0	0.0	0.0

ENERGY FLUX SPECTRUM E.N/CM**2.SEC.MEV

R	1.82E+00	3.64E+00	7.29E+00	1.28E+01	1.82E+01	2.73E+01	3.64E+01
	2.1950E+00	4.8881E-01	3.7771E-02	1.1537E-03	4.1515E-05	1.9149E-07	9.8107E-10

FN = 0 * EXP(MU * X)

MU*R =	1.00	2.00	4.00	7.00	10.00	15.00	20.00
	1.0005E+01	9.9961E+00	9.9941E+00	9.9904E+00	9.9868E+00	9.9807E+00	9.9748E+00

Fig. 12 Output print of the unscattered flux

```
  **  SCATTERED  FLUX  ***

RADIATION  ENERGY  = 0.1000E+02MEV

ANGULAR FLUXES OF RADIATION  N/CM**2.SEC.MEV.SR OR     IEF=1  E.N/CM**2.SEC.MEV.SR      IEF=  1
  W/R          4           7          13          22          31          46          61
 0.99312   7.4682E-03 5.4562E-03 1.4562E-03 1.2422E-04 8.6506E-06 8.4407E-08 7.3208E-10
 0.96397   7.6933E-03 5.4521E-03 1.3691E-03 1.0660E-04 6.7751E-06 5.6770E-08 4.2284E-10
 0.91223   8.1093E-03 5.4185E-03 1.2096E-03 7.8937E-05 4.2052E-06 2.6255E-08 1.4571E-10
 0.83911   8.7284E-03 5.3008E-03 9.7752E-04 4.7895E-05 1.9157E-06 7.4182E-09 2.5534E-11
 0.74633   9.5470E-03 4.9995E-03 6.8551E-04 2.1535E-05 5.5224E-07 1.0194E-09 1.6728E-12
 0.63605   1.0485E-02 4.3522E-03 3.7496E-04 5.8668E-06 7.4934E-08 4.3290E-11 2.2231E-14
 0.51086   1.1195E-02 3.1611E-03 1.2602E-04 6.2060E-07 2.4949E-09 2.0992E-13 1.5700E-17
 0.37370   9.8440E-03 1.3550E-03 1.2835E-05 7.3217E-09 3.4094E-12 7.8957E-18 1.6254E-23
 0.22778   4.7710E-03 1.1825E-04 3.6318E-08 1.2095E-13 3.2881E-19 1.4414E-28 5.6165E-38
 0.07652   7.1903E-06 3.0310E-11 2.6929E-22 4.4123E-39 5.9017E-56 0.0         0.0
-0.07652   0.0        0.0        0.0        0.0        0.0        0.0         0.0
-0.22778   0.0        0.0        0.0        0.0        0.0        0.0         0.0
-0.37370   0.0        0.0        0.0        0.0        0.0        0.0         0.0
-0.51086   0.0        0.0        0.0        0.0        0.0        0.0         0.0
-0.63605   0.0        0.0        0.0        0.0        0.0        0.0         0.0
-0.74663   0.0        0.0        0.0        0.0        0.0        0.0         0.0
-0.83911   0.0        0.0        0.0        0.0        0.0        0.0         0.0
-0.91223   0.0        0.0        0.0        0.0        0.0        0.0         0.0
-0.96397   0.0        0.0        0.0        0.0        0.0        0.0         0.0
-0.99312   0.0        0.0        0.0        0.0        0.0        0.0         0.0


ENERGY FLUX SPECTRUM  E.N/CM**2.SEC.MEV
 R          1.82E+00   3.64E+00   7.29E+00   1.28E+01   1.82E+01   2.73E+01   3.64E+01
         4.6980E-02 1.7272E-02 2.3314E-03 1.1575E-04 5.7552E-06 3.8727E-08 2.6069E-10


  FN - O * EXP( MU * X)
 MU*R =        1.00       2.00       4.00       7.00      10.00      15.00      20.00
         2.1415E-01 3.5321E-01 6.1689E-01 1.0023E+00 1.3845E+00 2.0185E+00 2.6505E+00
```

Fig. 13 Output print of the scattered flux at the source energy

REACTION RATE OR DOSE RATE(MR/H) ABOVE JJ-THE

R - MESH =	4	7	13	22	31	46	61
FDOS=	2.7209E-03	6.9285E-04	7.1440E-05	3.5771E-06	2.2395E-07	2.7968E-09	3.9974E-11
B-F =	1.298	1.484	1.981	3.247	5.649	15.293	42.665
FDOS=	2.7871E-03	7.0648E-04	7.2164E-05	3.5661E-06	2.2088E-07	2.7262E-09	3.8715E-11
B-F =	1.270	1.445	1.911	3.091	5.321	14.236	39.462
FDOS=	1.8180E-07	4.4291E-08	4.1822E-09	1.8375E-10	1.0244E-11	1.1134E-13	1.4699E-15
B-F =	1.234	1.350	1.650	2.373	3.676	8.662	22.320
FDOS=	1.3973E-07	3.4355E-08	3.3105E-09	1.5028E-10	8.6426E-12	9.7735E-14	1.3213E-15
B-F =	1.282	1.415	1.765	2.623	4.192	10.277	27.119

Fig. 14 Output print of the dose rates in mrem/h and their buildup factors, dose rates in mr/h and their buildup factors, energy absorptions in erg/g using energy transfer coefficient and their buildup factors and those using energy absorption coefficient and their buildup factors

```
                ********************
                *                  *
                *  INPUT DATA LIST *
                *                  *
                ********************

      ....*....1....*....2....*....3....*....4....*....5....*....6....*....7....*....8
 1     70 20 42                                                                        1
 2     LEAD(10 MEV)  PLANE ISOTROPIC  81-7-31,TEST OF HH PARAMETER OPTION              2
 3      4  0  0  0                                                                     3
 4      1 10 50  1  0                                                                 4
 5     42                                                                             5
 6      1 20  0                                                                       6
 7     10                                                                             7
 8     10.0       0.5                                                                 8
 9     70                                                                             9
10     41.91                                                                         10
11    820PB                                                                          11
12     2.7026     82.0      0.0330    11.34     0.088                                12
13      0  0  0                                                                      13
14      7  1  4  1  0                                                               14
15      4  7 13 22 31 46 61                                                         15
16     1.00       2.00      4.00      7.00      10.0      15.0      20.0            16
      ....*....1....*....2....*....3....*....4....*....5....*....6....*....7....*....8


      *** INPUT DATA END ***

MMX,MIQ,MJJ =    70    20    42

LTOT,LMAX,LRES =     131040     150000      18960
```

Fig. 15 List of input data for sample problem 2

```
                    OUTPUT OF THE COMPUTATION

RADIATION  ENERGY  = 0.1000E+02MEV

ENERGY FLUX SPECTRUM  E.N/CM**2.SEC.MEV
 R          1.82E+00    3.64E+00    7.29E+00    1.28E+01    1.82E+01    2.73E+01    3.64E+01
          0.0         0.0         0.0         0.0         0.0         0.0         0.0


  FN = 0 * EXP( MU * X)
 MU*R =        1.00        2.00        4.00        7.00       10.00       15.00       20.00
          0.0         0.0         0.0         0.0         0.0         0.0         0.0



RADIATION  ENERGY  = 0.9500E+01MEV

ENERGY FLUX SPECTRUM  E.N/CM**2.SEC.MEV
 R          1.82E+00    3.64E+00    7.29E+00    1.28E+01    1.82E+01    2.73E+01    3.64E+01
          1.3840E-05 4.0388E-06 4.0745E-07 1.5430E-08 6.3940E-10 3.4986E-12 2.0467E-14


  FN = 0 * EXP( MU * X)
 MU*R =        1.00        2.00        4.00        7.00       10.00       15.00       20.00
          3.7621E-05 2.9943E-05 2.2246E-05 1.6921E-05 1.4084E-05 1.1437E-05 9.9300E-06



RADIATION  ENERGY  = 0.9000E+01MEV

ENERGY FLUX SPECTRUM  E.N/CM**2.SEC.MEV
 R          1.82E+00    3.64E+00    7.29E+00    1.28E+01    1.82E+01    2.73E+01    3.64E+01
          3.7146E-05 1.0970E-05 1.1318E-06 4.4271E-08 1.8936E-09 1.0918E-11 6.7279E-14


  FN = 0 * EXP( MU * X)
 MU*R =        1.00        2.00        4.00        7.00       10.00       15.00       20.00
          1.0097E-04 8.1059E-05 6.1794E-05 4.8549E-05 4.1710E-05 3.5690E-05 3.2642E-05



RADIATION  ENERGY  = 0.8500E+01MEV

ENERGY FLUX SPECTRUM  E.N/CM**2.SEC.MEV
 R          1.82E+00    3.64E+00    7.29E+00    1.28E+01    1.82E+01    2.73E+01    3.64E+01
          7.0161E-05 2.1167E-05 2.2705E-06 9.3731E-08 4.2174E-09 2.6322E-11 1.7479E-13


  FN = 0 * EXP( MU * X)
 MU*R =        1.00        2.00        4.00        7.00       10.00       15.00       20.00
          1.9072E-04 1.5640E-04 1.2396E-04 1.0279E-04 9.2895E-05 8.6048E-05 8.4800E-05
```

Fig. 16 Output print of energy fluxes for the bremsstrahlung photons

REACTION RATE OR DOSE RATE(MR/H) ABOVE JJ-THE

R - MESH =	4	7	13	22	31	46	61
FDOS=	3.7044E-03	1.0707E-03	1.3182E-04	7.7480E-06	5.2563E-07	6.8070E-09	9.5652E-11
B-F =	1.767	2.294	3.654	7.032	13.258	37.222	102.092
FDOS=	3.7100E-03	1.0631E-03	1.2949E-04	7.5417E-06	5.0899E-07	6.5614E-09	9.1990E-11
B-F =	1.690	2.175	3.428	6.537	12.261	34.265	93.766
FDOS=	2.2480E-07	5.9635E-08	6.4744E-09	3.3496E-10	2.0925E-11	2.5042E-13	3.3813E-15
B-F =	1.526	1.818	2.554	4.325	7.509	19.482	51.347
FDOS=	1.8040E-07	4.8805E-08	5.4597E-09	2.9162E-10	1.8611E-11	2.2744E-13	3.1041E-15
B-F =	1.655	2.010	2.911	5.090	9.027	23.916	63.710

Fig. 17 Output print of the total dose rates (contributed from the primary gamma rays and from the bremsstrahlung photons) and total energy absorptions as well as their total buildup factors

```
J, PHOTON ENERGY(MEV) :  32  9.829E-02
MU*R =        1.00        2.00        4.00        7.00       10.00       15.00       20.00
       9.4947E-03 6.6404E-03 4.9956E-03 4.7501E-03 5.5855E-03 9.4976E-03 1.9376E-02

J, PHOTON ENERGY(MEV) :  33  8.967E-02
MU*R =        1.00        2.00        4.00        7.00       10.00       15.00       20.00
       1.4711E-02 1.0254E-02 7.6622E-03 7.1974E-03 8.3359E-03 1.3752E-02 2.7161E-02

J, PHOTON ENERGY(MEV) :  34  8.243E-02
MU*R =        1.00        2.00        4.00        7.00       10.00       15.00       20.00
       2.2153E-02 1.5408E-02 1.1461E-02 1.0684E-02 1.2268E-02 1.9925E-02 3.8748E-02

J, PHOTON ENERGY(MEV) :  35  7.628E-02
MU*R =        1.00        2.00        4.00        7.00       10.00       15.00       20.00
       1.9144E-02 1.3340E-02 9.9655E-03 9.3644E-03 1.0847E-02 1.7855E-02 3.5049E-02

J, PHOTON ENERGY(MEV) :  36  7.098E-02
MU*R =        1.00        2.00        4.00        7.00       10.00       15.00       20.00
       1.9267E-02 1.3412E-02 9.9926E-03 9.3369E-03 1.0739E-02 1.7452E-02 3.3878E-02

J, PHOTON ENERGY(MEV) :  37  6.637E-02
MU*R =        1.00        2.00        4.00        7.00       10.00       15.00       20.00
       1.7322E-02 1.2070E-02 9.0113E-03 8.4452E-03 9.7413E-03 1.5896E-02 3.0946E-02

J, PHOTON ENERGY(MEV) :  38  6.233E-02
MU*R =        1.00        2.00        4.00        7.00       10.00       15.00       20.00
       1.1129E-02 7.8131E-03 5.9255E-03 5.6967E-03 6.7432E-03 1.1423E-02 2.2833E-02

J, PHOTON ENERGY(MEV) :  39  5.874E-02
MU*R =        1.00        2.00        4.00        7.00       10.00       15.00       20.00
       1.0940E-02 7.6545E-03 5.7619E-03 5.4691E-03 6.3874E-03 1.0607E-02 2.0897E-02

J, PHOTON ENERGY(MEV) :  40  5.466E-02
MU*R =        1.00        2.00        4.00        7.00       10.00       15.00       20.00
       9.5714E-03 6.6761E-03 4.9942E-03 4.6934E-03 5.4277E-03 8.8903E-03 1.7355E-02

J, PHOTON ENERGY(MEV) :  41  5.085E-02
MU*R =        1.00        2.00        4.00        7.00       10.00       15.00       20.00
       7.2954E-03 5.1157E-03 3.8683E-03 3.6964E-03 4.3442E-03 7.2731E-03 1.4405E-02

J, PHOTON ENERGY(MEV) :  42  4.754E-02
MU*R =        1.00        2.00        4.00        7.00       10.00       15.00       20.00
       5.6813E-03 3.9843E-03 3.0134E-03 2.8799E-03 3.3847E-03 5.6667E-03 1.1223E-02
```

Fig. 18 Output print of energy spectra in terms of $\exp(\mu x)I(x,E)$ at 7 spatial meshes

```
          ********************
          *                  *
          *  INPUT DATA LIST *
          *                  *
          ********************

     ....*....1....*....2....*....3....*....4....*....5....*....6....*....7....*....8
1      0  0  0
2    CF-S AIR CONCR AIR 56-5-13, TEST OF PALPSB
3      1  2  0  0
4      2  0  1  0  1
5     27 27 45
6      6 20  1
7      0  3
8     14.20       0.10        1.000E 09
9      3  9 21 21  6 31
10    1.00        4.00        75.00      100.0      500.0      15000.0
11    1.00        1.00         1.00
12    10200
13    0.005
14     2  2  2  4  2  2
15     1  1  1  4  1  1
16   AIR
17   N
18    1074 14.00       4.010E-05
19   OXY
20    1086 16.00       1.050E-05
21   CONC
22   HY
23    1011 1.000       0.01213
24   OXY
25    1086 16.000      0.04982
26   SI
27    1140 28.00       0.01527
28   CA
29    1200 40.0        0.00375
30     0
31    10  0  1
32     3 17 25 33 38 46 54 60 71 81
33   DOSE RATE
34    0.150      0.1490     0.1480     0.1475     0.1472     0.1471     0.1470     0.1468
35    0.1466     0.1464     0.1462     0.1460     0.1459     0.1457     0.1454     0.1452
36    0.1450     0.1420     0.1400     0.1380     0.1360     0.1330     0.1310     0.1290
37    0.1270     0.1220     0.1170     0.1150     0.1060     0.1000     0.093      0.087
38   DOSE RATE
39    0.1500     0.1490     0.1490     0.1480     0.1470     0.1460     0.1455     0.1450
40    0.1430     0.14000     0.1350    0.1310     0.1270     0.1170     0.1060     0.093
41    0.080      0.068      0.0590     0.0505     0.0430     0.0370     0.033      0.028
42    0.0240     0.0206     0.0176     0.0150     0.0130     0.0110     0.0094     0.0081
43   DOSE RATE
44    0.150      0.149      0.147      0.1455     0.1430     0.1360     0.1270     0.1180
45    0.0800     0.0600     0.04350    0.03300    0.02350    0.01740    0.01280    0.0094
46    0.0068     0.0050     0.0037     0.00368     0.00367     0.00368     0.0037     0.0037
47    0.00375    0.00380    0.00385    0.00392    0.00410    0.00420    0.00420    0.00420
48    0.00420    0.00425    0.00430    0.00430    0.00430    0.00435    0.00440    0.0045
49    0.0045     0.0045     0.0044     0.0044     0.00385
     ....*....1....*....2....*....3....*....4....*....5....*....6....*....7....*....8

     *** INPUT DATA END ***
```

Fig. 19 List of input data for smaple problem 3

```
                    INPUT  DATA
***CF-S AIR CONCR AIR 56-5-13, TEST OF PALPSB                              ***

KNDG,KIN,NORF,KTST  =    1    2    0    0

NGEOM,MONOE,MNOORE,IBREM,IPRNT =    2    0    1    0    1

          ONE DIMENSIONAL SPHERICAL GEOMETRY


  ENERGY MESH =  27    MATERIAL REGION =  6    ANGULAR MESH = 20    FISSION = 1    JSTAT= 0

   NBND =  0    MSR =  3    IQIQ = 0    JOTAL = 0

   E-MAX = 1.420E+01 MEV    LETHARGY WIDTH = 1.000E-01  SOURCE NORM. = 1.000E+09  RDST = 0.0
   E(MEV) = 1.420E+01 1.285E+01 1.163E+01 1.052E+01 9.519E+00 8.613E+00 7.793E+00 7.052E+00 6.380E+00 5.773E+00
   E(MEV) = 5.224E+00 4.727E+00 4.277E+00 3.870E+00 3.502E+00 3.168E+00 2.867E+00 2.594E+00 2.347E+00 2.124E+00
   E(MEV) = 1.922E+00 1.739E+00 1.573E+00 1.424E+00 1.288E+00 1.166E+00 1.055E+00

REGION              1         2         3         4         5         6         7         8         9         10
   MESHES =         3         9        21        21         6        31
   THICKNESS =  1.000E+00 4.000E+00 7.500E+01 1.000E+02 5.000E+02 1.500E+04

ANGULAR QUADATURE CONSTANTS COSINE AND WEIGHT
 W-P=   0.99312   0.96397   0.91223   0.83911   0.74633   0.63605   0.51086   0.37370   0.22778   0.07652
 W-P=  -0.07652  -0.22778  -0.37370  -0.51086  -0.63605  -0.74663  -0.83911  -0.91223  -0.96397  -0.99312
WW-P=   0.01761   0.04060   0.06267   0.08328   0.10193   0.11819   0.13169   0.14210   0.14917   0.15275
WW-P=   0.15275   0.14917   0.14210   0.13169   0.11819   0.10193   0.08328   0.06267   0.04060   0.01761

NO OF ELEMENTS IN EACH REGION=  2  2  2  4  2  2

IDENTIFICATION OF REGION=  1  1  1  4  1  1

SOURCE S(R,E)=S(R)*S(E)/4*3.14
SR(N) = 0.100E+01 0.100E+01 0.100E+01
SE(N) = 0.340E-04 0.101E-03 0.268E-03 0.642E-03 0.140E-02 0.279E-02 0.517E-02 0.896E-02 0.146E-01 0.225E-01 0.330E-01 0.463E-01
SE(N) = 0.624E-01 0.812E-01 0.102E+00 0.125E+00 0.150E+00 0.175E+00 0.199E+00 0.224E+00 0.247E+00 0.268E+00 0.287E+00 0.304E+00
SE(N) = 0.319E+00 0.331E+00 0.340E+00
 TOTAL SOURCE INTENSITY = 4.0724E+00
 NORMALIZED SOURCE INTENSITY
 SR= 0.2456E+09 0.2456E+09 0.2456E+09
RMES(CM)= 3.333E-01 6.667E-01 1.000E+00 1.000E+00 1.500E+00 2.000E+00 2.500E+00 3.000E+00 3.500E+00 4.000E+00
RMES(CM)= 4.500E+00 5.000E+00 5.000E+00 8.750E+00 1.250E+01 1.625E+01 2.000E+01 2.375E+01 2.750E+01 3.125E+01
RMES(CM)= 3.500E+01 3.875E+01 4.250E+01 4.625E+01 5.000E+01 5.375E+01 5.750E+01 6.125E+01 6.500E+01 6.875E+01
RMES(CM)= 7.250E+01 7.625E+01 8.000E+01 8.000E+01 8.500E+01 9.000E+01 9.500E+01 1.000E+02 1.050E+02 1.100E+02
RMES(CM)= 1.150E+02 1.200E+02 1.250E+02 1.300E+02 1.350E+02 1.400E+02 1.450E+02 1.500E+02 1.550E+02 1.600E+02
RMES(CM)= 1.650E+02 1.700E+02 1.750E+02 1.800E+02 1.800E+02 2.800E+02 3.800E+02 4.800E+02 5.800E+02 6.800E+02
RMES(CM)= 6.800E+02 1.180E+03 1.680E+03 2.180E+03 2.680E+03 3.180E+03 3.680E+03 4.180E+03 4.680E+03 5.180E+03
RMES(CM)= 5.680E+03 6.180E+03 6.680E+03 7.180E+03 7.680E+03 8.180E+03 8.680E+03 9.180E+03 9.680E+03 1.018E+04
RMES(CM)= 1.068E+04 1.118E+04 1.168E+04 1.218E+04 1.268E+04 1.318E+04 1.368E+04 1.418E+04 1.468E+04 1.518E+04
RMES(CM)= 1.568E+04

RADIUS(CM)=
RD= 3.333E-01 6.667E-01 1.000E+00 1.500E+00 2.000E+00 2.500E+00 3.000E+00 3.500E+00 4.000E+00 4.500E+00
RD= 5.000E+00 8.750E+00 1.250E+01 1.625E+01 2.000E+01 2.375E+01 2.750E+01 3.125E+01 3.500E+01 3.875E+01
RD= 4.250E+01 4.625E+01 5.000E+01 5.375E+01 5.750E+01 6.125E+01 6.500E+01 6.875E+01 7.250E+01 7.625E+01
RD= 8.000E+01 8.500E+01 9.000E+01 9.500E+01 1.000E+02 1.050E+02 1.100E+02 1.150E+02 1.200E+02 1.250E+02
RD= 1.300E+02 1.350E+02 1.400E+02 1.450E+02 1.500E+02 1.550E+02 1.600E+02 1.650E+02 1.700E+02 1.750E+02
RD= 1.800E+02 2.800E+02 3.800E+02 4.800E+02 5.800E+02 6.800E+02 1.180E+03 1.680E+03 2.180E+03 2.680E+03
RD= 3.180E+03 3.680E+03 4.180E+03 4.680E+03 5.180E+03 5.680E+03 6.180E+03 6.680E+03 7.180E+03 7.680E+03
RD= 8.180E+03 8.680E+03 9.180E+03 9.680E+03 1.018E+04 1.068E+04 1.118E+04 1.168E+04 1.218E+04 1.268E+04
RD= 1.316E+04 1.368E+04 1.418E+04 1.468E+04 1.518E+04 1.568E+04 0.0       0.0       0.0       0.0
```

Fig. 20(a) List of input and constants used in the calculation

```
RO= 0.0

DR(CM)= 3.333E-01 5.000E-01 3.750E+00 5.000E+00 1.000E+02 5.000E+02


***** NUCLEAR DATA   *****

   MATERIAL =AIR                                NUCLIDE =N

   TITLE =N-14 0.1U
  MAXG/JFMU/LL =     50     26     11
  MAS NO. = 14.00            ATOMIC DENSITY =0.4010E-04
SIGMA-T =  1.570       1.569       1.421       1.414       1.296       1.257       1.471       1.305       1.381       1.399
SIGMA-T =  1.406       1.327       1.967       1.826       1.675       1.665       1.476       1.422       1.505       1.553
SIGMA-T =  1.650       2.119       2.127       2.283       1.816       1.931       2.193
 SIG-C = 0.1616E-04 0.1880E-04 0.1918E-04 0.2157E-04 0.1910E-04 0.1568E-04 0.1832E-04 0.1375E-04 0.1611E-04 0.2247E-04
 SIG-C = 0.1539E-04 0.1165E-04 0.1843E-04 0.2325E-04 0.2539E-04 0.2226E-04 0.1442E-04 0.1699E-04 0.2171E-04 0.2598E-04
 SIG-C = 0.2985E-04 0.3334E-04 0.3601E-04 0.3673E-04 0.3530E-04 0.3220E-04 0.2810E-04
SIGMA-S= 0.8886      0.9027      0.8114      0.8954      0.8986      0.8800      1.077       0.9649      1.074       1.168
SIGMA-S=  1.137      0.9772      1.543       1.433       1.288       1.336       1.222       1.265       1.389       1.453
SIGMA-S=  1.581       2.019       2.072       2.115       1.765       1.920       2.185

INEL. MATRIX

   MATERIAL =AIR                                NUCLIDE =OXY

   TITLE =O-16 0.1U
  MAXG/JFMU/LL =     50     50     11
  MAS NO. = 16.00            ATOMIC DENSITY =0.1050E-04
SIGMA-T =  1.643       1.569       1.685       1.356       1.225       1.269       1.198       1.182       0.9666      1.379
SIGMA-T =  1.387       1.342       1.877       2.642       3.154       2.197       1.150       1.078       0.6132      1.381
SIGMA-T =  2.181       1.826       2.175       2.440       4.115       2.934       5.426
 SIG-C = 0.7545E-08 0.7930E-08 0.8336E-08 0.8758E-08 0.9203E-08 0.9669E-08 0.1016E-07 0.1068E-07 0.1123E-07 0.1181E-07
 SIG-C = 0.1241E-07 0.1304E-07 0.1370E-07 0.1440E-07 0.1514E-07 0.1592E-07 0.1674E-07 0.1758E-07 0.1849E-07 0.1943E-07
 SIG-C = 0.2043E-07 0.2148E-07 0.2257E-07 0.2373E-07 0.2495E-07 0.2623E-07 0.2756E-07
SIGMA-S= 0.9779      1.021       1.134       0.9316      0.8366      0.8927      0.9059      0.9789      0.8839      1.348
SIGMA-S=  1.304      1.271       1.786       2.619       3.152       2.196       1.150       1.078       0.6132      1.381
SIGMA-S=  2.181      1.826       2.175       2.440       4.115       2.934       5.426

INEL. MATRIX

SIGMA-TOTAL( 1/CM)       REGION NO.=  1
 8.02194E-05  7.94161E-05  7.46821E-05  7.09306E-05  6.48292E-05  6.37487E-05  7.15631E-05  6.47523E-05  6.55392E-05  7.06011E-05
 7.09523E-05  6.73171E-05  9.85955E-05  1.00976E-04  1.00288E-04  8.98140E-05  7.12695E-05  6.83515E-05  6.67983E-05  7.67639E-05
 8.90475E-05  1.04167E-04  1.08133E-04  1.17155E-04  1.16029E-04  1.08257E-04  1.44894E-04

SIGMA-TOTAL( 1/CM)       REGION NO.=  2
 8.02194E-05  7.94161E-05  7.46821E-05  7.09306E-05  6.48292E-05  6.37487E-05  7.15631E-05  6.47523E-05  6.55392E-05  7.06011E-05
 7.09523E-05  6.73171E-05  9.85955E-05  1.00976E-04  1.00288E-04  8.98140E-05  7.12695E-05  6.83515E-05  6.67983E-05  7.67639E-05
 8.90475E-05  1.04167E-04  1.08133E-04  1.17155E-04  1.16029E-04  1.08257E-04  1.44894E-04

SIGMA-TOTAL( 1/CM)       REGION NO.=  3
 8.02194E-05  7.94161E-05  7.46821E-05  7.09306E-05  6.48292E-05  6.37487E-05  7.15631E-05  6.47523E-05  6.55392E-05  7.06011E-05
 7.09523E-05  6.73171E-05  9.85955E-05  1.00976E-04  1.00288E-04  8.98140E-05  7.12695E-05  6.83515E-05  6.67983E-05  7.67639E-05
 8.90475E-05  1.04167E-04  1.08133E-04  1.17155E-04  1.16029E-04  1.08257E-04  1.44894E-04

   MATERIAL =CONC                               NUCLIDE =HY

   TITLE =H-1 0.1U
  MAXG/JFMU/LL =     50      0      1
  MAS NO. = 1.000            ATOMIC DENSITY =0.1213E-01
SIGMA-T = 0.6894      0.7573      0.8300      0.9074      0.9892      1.076       1.168       1.266       1.368       1.477
```

Fig. 20(b) List of input and constants used in the calculation

```
SIGMA-T =  1.589      1.705      1.825      1.951      2.082      2.219      2.361      2.505      2.658      2.817
SIGMA-T =  2.985      3.158      3.340      3.530      3.725      3.930      4.142
 SIG-C = 0.2969E-04 0.3043E-04 0.3141E-04 0.3223E-04 0.3297E-04 0.3359E-04 0.3425E-04 0.3514E-04 0.3556E-04 0.3594E-04
 SIG-C = 0.3627E-04 0.3636E-04 0.3628E-04 0.3617E-04 0.3595E-04 0.3576E-04 0.3548E-04 0.3508E-04 0.3473E-04 0.3441E-04
 SIG-C = 0.3427E-04 0.3428E-04 0.3432E-04 0.3436E-04 0.3445E-04 0.3443E-04 0.3443E-04
SIGMA-S= 0.6894     0.7573     0.8300     0.9074     0.9892     1.076      1.168      1.266      1.368      1.477
SIGMA-S=  1.589      1.705      1.825      1.951      2.082      2.219      2.361      2.505      2.658      2.817
SIGMA-S=  2.985      3.158      3.340      3.530      3.725      3.930      4.142

   MATERIAL =CONC                              NUCLIDE =OXY

   TITLE =O-16 0.1U
  MAXG/JFMU/LL =     50     50     11
  MAS NO. = 16.00            ATOMIC DENSITY =0.4982E-01
SIGMA-T =  1.643      1.569      1.685      1.356      1.225      1.269      1.198      1.182      0.9666     1.379
SIGMA-T =  1.387      1.342      1.877      2.642      3.154      2.197      1.150      1.078      0.6132     1.381
SIGMA-T =  2.181      1.826      2.175      2.440      4.115      2.934      5.426
 SIG-C = 0.7545E-08 0.7930E-08 0.8336E-08 0.8758E-08 0.9203E-08 0.9669E-08 0.1016E-07 0.1068E-07 0.1123E-07 0.1181E-07
 SIG-C = 0.1241E-07 0.1304E-07 0.1370E-07 0.1440E-07 0.1514E-07 0.1592E-07 0.1674E-07 0.1758E-07 0.1849E-07 0.1943E-07
 SIG-C = 0.2043E-07 0.2148E-07 0.2257E-07 0.2373E-07 0.2495E-07 0.2623E-07 0.2756E-07
SIGMA-S= 0.9779     1.021      1.134      0.9316     0.8366     0.8927     0.9059     0.9789     0.8839     1.348
SIGMA-S=  1.304      1.271      1.786      2.619      3.152      2.196      1.150      1.078      0.6132     1.381
SIGMA-S=  2.181      1.826      2.175      2.440      4.115      2.934      5.426

INEL. MATRIX

   MATERIAL =CONC                              NUCLIDE =SI

   TITLE =SI-0 0.1U
  MAXG/JFMU/LL =     50     50     11
  MAS NO. = 28.00            ATOMIC DENSITY =0.1527E-01
SIGMA-T =  1.813      1.846      1.820      1.799      1.822      1.911      1.997      1.958      1.955      2.220
SIGMA-T =  2.109      2.566      2.291      2.103      2.074      2.409      2.455      2.964      2.476      2.687
SIGMA-T =  4.041      2.487      3.465      2.823      2.696      2.617      3.397
 SIG-C = 0.5026E-03 0.5199E-03 0.5349E-03 0.5466E-03 0.5584E-03 0.5744E-03 0.5800E-03 0.5888E-03 0.5957E-03 0.6052E-03
 SIG-C = 0.6105E-03 0.6168E-03 0.6200E-03 0.6259E-03 0.6300E-03 0.6390E-03 0.6400E-03 0.6400E-03 0.6413E-03 0.6497E-03
 SIG-C = 0.6505E-03 0.6500E-03 0.6500E-03 0.6533E-03 0.6599E-03 0.6600E-03 0.6597E-03
SIGMA-S= 0.7314     0.7472     0.7122     0.6842     0.7257     0.8125     0.8737     0.9026     0.9693     1.303
SIGMA-S=  1.298      1.864      1.638      1.488      1.498      1.863      1.961      2.546      2.132      2.407
SIGMA-S=  3.908      2.470      3.451      2.816      2.695      2.616      3.396

INEL. MATRIX

   MATERIAL =CONC                              NUCLIDE =CA

   TITLE =CA-0 0.1U
  MAXG/JFMU/LL =     50     50     11
  MAS NO. = 40.00            ATOMIC DENSITY =0.3750E-02
SIGMA-T =  2.146      2.268      2.399      2.528      2.688      2.770      2.891      2.998      3.072      3.232
SIGMA-T =  3.316      3.423      3.652      3.691      3.689      3.293      3.669      3.632      3.341      3.139
SIGMA-T =  3.123      3.044      2.714      1.967      2.490      2.497      2.324
 SIG-C = 0.1336E-04 0.1450E-04 0.1573E-04 0.1708E-04 0.1811E-04 0.1878E-04 0.1937E-04 0.2042E-04 0.2490E-04 0.3005E-04
 SIG-C = 0.3466E-04 0.4158E-04 0.5121E-04 0.6176E-04 0.7199E-04 0.8389E-04 0.9518E-04 0.1049E-03 0.1157E-03 0.1275E-03
 SIG-C = 0.1403E-03 0.1540E-03 0.1691E-03 0.1857E-03 0.2036E-03 0.2236E-03 0.2456E-03
SIGMA-S= 0.8825     0.9504     1.073      1.182      1.314      1.400      1.532      1.668      1.789      2.020
SIGMA-S=  2.203      2.386      2.743      3.041      3.206      2.928      3.414      3.473      3.243      3.078
SIGMA-S=  3.086      3.016      2.696      1.956      2.481      2.493      2.320

INEL. MATRIX

SIGMA-TOTAL( 1/CM)      REGION NO.=  4
 1.25949E-01  1.24063E-01  1.30775E-01  1.15527E-01  1.10926E-01  1.15863E-01  1.15180E-01  1.15384E-01  1.06131E-01  1.32648E-01
```

Fig. 20(c) List of input and constants used in the calculation

```
 1.32986E-01  1.39537E-01  1.64343E-01  2.01263E-01  2.27907E-01  1.85484E-01  1.37193E-01  1.42985E-01  1.13127E-01  1.55762E-01
 2.18278E-01  1.78691E-01  2.11955E-01  2.14882E-01  3.00715E-01  2.43161E-01  3.81160E-01

SIGMA-TOTAL( 1/CM)      REGION NO.=  5
 8.02194E-05  7.94161E-05  7.46821E-05  7.09306E-05  6.48292E-05  6.37487E-05  7.15631E-05  6.47523E-05  6.55392E-05  7.06011E-05
 7.09523E-05  6.73171E-05  9.85955E-05  1.00976E-04  1.00288E-04  8.98140E-05  7.12695E-05  6.83515E-05  6.67983E-05  7.67639E-05
 8.90475E-05  1.04167E-04  1.08133E-04  1.17155E-04  1.16029E-04  1.08257E-04  1.44894E-04

SIGMA-TOTAL( 1/CM)      REGION NO.=  6
 8.02194E-05  7.94161E-05  7.46821E-05  7.09306E-05  6.48292E-05  6.37487E-05  7.15631E-05  6.47523E-05  6.55392E-05  7.06011E-05
 7.09523E-05  6.73171E-05  9.85955E-05  1.00976E-04  1.00288E-04  8.98140E-05  7.12695E-05  6.83515E-05  6.67983E-05  7.67639E-05
 8.90475E-05  1.04167E-04  1.08133E-04  1.17155E-04  1.16029E-04  1.08257E-04  1.44894E-04

MRK,MRKK,IDOS,IEF,ICUR =   10    0    1    0    0

 NAME OF RESPONSE = FLUX TO MREM/HR CONVERSION FACTOR ( ANSI/ANS-6.1.1-1977 )
DOSE CON.= 0.2100E+00 0.1890E+00 0.1720E+00 0.1560E+00 0.1470E+00 0.1470E+00 0.1470E+00 0.1470E+00 0.1490E+00 0.1520E+00
DOSE CON.= 0.1540E+00 0.1520E+00 0.1490E+00 0.1430E+00 0.1400E+00 0.1350E+00 0.1320E+00 0.1280E+00 0.1260E+00 0.1280E+00
DOSE CON.= 0.1290E+00 0.1300E+00 0.1300E+00 0.1310E+00 0.1310E+00 0.1320E+00 0.1320E+00

 NAME OF RESPONSE = DOSE RATE

 NAME OF RESPONSE =
DOSE CON.= 0.1500E+00 0.1490E+00 0.1480E+00 0.1475E+00 0.1472E+00 0.1471E+00 0.1470E+00 0.1468E+00 0.1466E+00 0.1464E+00
DOSE CON.= 0.1462E+00 0.1460E+00 0.1459E+00 0.1457E+00 0.1454E+00 0.1452E+00 0.1450E+00 0.1420E+00 0.1400E+00 0.1380E+00
DOSE CON.= 0.1360E+00 0.1330E+00 0.1310E+00 0.1290E+00 0.1270E+00 0.1220E+00 0.1170E+00
```

Fig. 20(d) List of input and constants used in the calculation

OUTPUT OF THE COMPUTATION

RADIATION ENERGY = 0.1420E+02MEV

ANGULAR FLUXES OF RADIATION N/CM**2.SEC.MEV.SR OR IEF=1 E.N/CM**2.SEC.MEV.SR IEF= 0

M/R	3	17	25	33	38	46	54	60	71	81
0.99312	1.3153E+03	4.7415E+01	7.5717E+00	2.9519E+00	2.5083E-01	2.2567E-03	2.4081E-05	1.6335E-06	1.6929E-08	3.4637E-09
0.96397	1.2757E+03	0.0	0.0	0.0	0.0	0.0	0.0	0.0	0.0	0.0
0.91223	1.2052E+03	0.0	0.0	0.0	0.0	0.0	0.0	0.0	0.0	0.0
0.83911	1.1016E+03	0.0	0.0	0.0	0.0	0.0	0.0	0.0	0.0	0.0
0.74633	9.7857E+02	0.0	0.0	0.0	0.0	0.0	0.0	0.0	0.0	0.0
0.63605	8.4471E+02	0.0	0.0	0.0	0.0	0.0	0.0	0.0	0.0	0.0
0.51086	6.7845E+02	0.0	0.0	0.0	0.0	0.0	0.0	0.0	0.0	0.0
0.37370	4.9629E+02	0.0	0.0	0.0	0.0	0.0	0.0	0.0	0.0	0.0
0.22778	3.0250E+02	0.0	0.0	0.0	0.0	0.0	0.0	0.0	0.0	0.0
0.07652	1.0162E+02	0.0	0.0	0.0	0.0	0.0	0.0	0.0	0.0	0.0
-0.07652	0.0	0.0	0.0	0.0	0.0	0.0	0.0	0.0	0.0.	0.0
-0.22778	0.0	0.0	0.0	0.0	0.0	0.0	0.0	0.0	0.0	0.0
-0.37370	0.0	0.0	0.0	0.0	0.0	0.0	0.0	0.0	0.0	0.0
-0.51086	0.0	0.0	0.0	0.0	0.0	0.0	0.0	0.0	0.0	0.0
-0.63605	0.0	0.0	0.0	0.0	0.0	0.0	0.0	0.0	0.0	0.0
-0.74663	0.0	0.0	0.0	0.0	0.0	0.0	0.0	0.0	0.0	0.0
-0.83911	0.0	0.0	0.0	0.0	0.0	0.0	0.0	0.0	0.0	0.0
-0.91223	0.0	0.0	0.0	0.0	0.0	0.0	0.0	0.0	0.0	0.0
-0.96397	0.0	0.0	0.0	0.0	0.0	0.0	0.0	0.0	0.0	0.0
-0.99312	0.0	0.0	0.0	0.0	0.0	0.0	0.0	0.0	0.0	0.0

SCALAR FLUX N/CM**2.SEC.MEV

R	1.00E+00	2.00E+01	5.00E+01	8.00E+01	1.00E+02	1.40E+02	1.80E+02	6.80E+02	5.68E+03	1.07E+04
	4.1615E+03	5.2463E+00	8.3778E-01	3.2662E-01	2.7753E-02	2.4970E-04	2.6645E-06	1.8074E-07	1.8731E-09	3.8325E-10

RADIATION ENERGY = 0.1285E+02MEV

ANGULAR FLUXES OF RADIATION N/CM**2.SEC.MEV.SR OR IEF=1 E.N/CM**2.SEC.MEV.SR IEF= 0

M/R	3	17	25	33	38	46	54	60	71	81
0.99312	3.9173E+03	1.0221E+02	1.6322E+01	6.3633E+00	5.5141E-01	5.1595E-03	5.7258E-05	7.5095E-06	7.7747E-08	1.5892E-08
0.96397	3.7971E+03	4.5114E-03	1.9990E-03	1.4362E-03	4.8470E-03	2.4763E-04	5.2519E-06	3.7157E-08	3.7076E-10	1.5743E-10
0.91223	3.5826E+03	2.1174E-03	1.2174E-03	9.0383E-04	1.7569E-02	4.1364E-04	6.1432E-06	2.3820E-09	2.0061E-10	8.7394E-11
0.83911	3.2681E+03	1.0793E-03	7.0721E-04	5.3036E-04	1.0595E-02	1.8142E-04	2.2105E-06	8.7555E-10	8.6136E-11	3.6709E-11
0.74633	2.9032E+03	7.2937E-04	4.6322E-04	3.5995E-04	2.8295E-03	3.9749E-05	4.4715E-07	4.0822E-10	3.5310E-11	1.3897E-11
0.63605	2.5159E+03	6.1382E-04	3.8493E-04	3.5034E-04	2.3327E-03	2.4868E-05	2.7383E-07	2.5897E-10	2.2206E-11	8.7002E-12
0.51086	2.0207E+03	5.2518E-04	3.3232E-04	4.3448E-04	1.7821E-03	1.6910E-05	1.8485E-07	1.7567E-10	1.4436E-11	5.3992E-12
0.37370	1.4782E+03	4.8283E-04	2.9794E-04	1.0725E-03	1.2975E-03	1.2573E-05	1.4030E-07	1.2694E-10	9.3070E-12	3.5674E-12
0.22778	9.0098E+02	4.4011E-04	2.8099E-04	4.1625E-03	8.2847E-04	7.7057E-06	8.3173E-08	7.8207E-11	5.3852E-12	1.9271E-12
0.07652	3.0268E+02	4.0606E-04	2.6750E-04	4.1573E-03	6.6229E-04	6.4153E-06	6.8919E-08	3.8828E-11	2.1317E-12	7.3358E-13
-0.07652	3.1608E-03	3.8890E-04	2.6075E-04	4.1563E-03	3.8003E-04	3.6090E-06	7.3078E-11	2.2292E-11	7.5454E-13	2.1965E-13
-0.22778	2.2681E-03	3.8652E-04	2.6270E-04	1.6722E-03	1.5573E-04	1.7748E-06	5.5203E-11	1.7184E-11	3.1304E-13	4.6000E-14
-0.37370	1.6697E-03	3.8917E-04	2.7033E-04	4.6471E-04	4.2157E-05	3.9381E-07	0.0	0.0	0.0	0.0
-0.51086	1.2832E-03	3.9611E-04	2.8331E-04	3.4684E-04	3.0972E-05	2.9587E-07	0.0	0.0	0.0	0.0
-0.63605	1.0231E-03	4.0522E-04	2.9987E-04	2.2005E-04	1.8993E-05	1.7415E-07	0.0	0.0	0.0	0.0
-0.74663	8.3329E-04	4.1623E-04	3.2024E-04	2.2665E-04	1.9358E-05	1.7496E-07	0.0	0.0	0.0	0.0
-0.83911	6.9804E-04	4.2870E-04	3.4529E-04	2.9351E-04	2.5352E-05	2.3259E-07	0.0	0.0	0.0	0.0
-0.91223	6.0020E-04	4.4233E-04	3.7735E-04	3.0498E-04	2.6251E-05	2.3973E-07	0.0	0.0	0.0	0.0
-0.96397	5.3556E-04	4.5678E-04	4.1656E-04	3.7518E-04	3.2389E-05	2.9691E-07	0.0	0.0	0.0	0.0

Fig. 21 Output print of angular and scalar fluxes at 10 spatial meshes